Journal Name

ARTICLE

Miracle Molecule of Pyrene-based Aggregation-induced Emission Luminogens and their Applications

Received 00th January 20xx,
Accepted 00th January 20xx

DOI: 10.1039/x0xx00000x

www.rsc.org/

Md. Monarul Islam,[abc] Zhen Hu,[a] Qingsong Wang,[a] Carl Redshaw[d] Xing Feng,*[ab]

"Unity is force"-Aesop. It is a common phenomenon that traditional chromophores exhibit high fluorescence in dilute solution but luminescence is quenched at high concentrations or in the aggregate state, ie "aggregation-caused quenching" (ACQ). Tang reported the unusual photophysical observation that found in a group of luminogens can exhibit weak or no fluorescence in solution yet are highly emissive in the aggregate or solid state, which is defined as aggregation-induced emission (AIE).This discovery of AIE helped solve the ACQ effect in traditional luminophores. Pyrene is an important polycyclic aromatic hydrocarbon (PAH), which exhibits very different photophysical behaviour in solution versus the aggregate state, and the ACQ effect has played a dominant role in pyrene chemistry. The ACQ effect is harmful to some practical applications and is a challenge in organic light-emitting diodes (OLEDs) and light-emitting electrochemical cells for which the effect is more severe in the solid state. Thus, how to overcome the ACQ effect observed in pyrene chemistry still remains a challenge. In this review, novel strategies to transform pyrene-based ACQ luminogens to AIE luminogens are summarized, following the basicAIE work mechanics—restriction of intramolecular rotation (RIR). Furthermore, prospective applications of pyrene-based AIEgens are discussed as is the potential for designing and synthesising new organic functional materials.

1. Introduction

1.1 Chemistry of pyrene and its derivatives

Pyrene is a representative member of the polycyclic aromatic hydrocarbons (PAHs), and consists of four fused benzene rings with extensive π-electron delocalization. Since Weitzenböck first synthesized pyrene **1** in the laboratory in 1913, pyrene **1** (Fig. 1) and its derivatives have attracted much attention of scientists, primarily due to their blue emissive property, good hole-transporting ability and their application in organic electronics, such as organic light-emitting diodes (OLEDs), light-emitting electrochemical materials, solar cells etc.[1-3]Salient features of pyrene are that its π -system does not require protection during functionalization,[4] their moderately long fluorescence lifetimes, and excimer formation.[5] However, there are two major drawbacks of pyrenes when used in organic fluorescent materials,(i) the absorption and emission of the pyrene fluorophore lies in the near-UV region, whereas a good optoelectronic device emits in the visible region and (ii) excimer formation occurs in concentrated solutions or in the solid state which decreases or quenches the fluorescence intensity, with a the large red-shifted emission.[6-8]This common phenomenon is defined as aggregation-induced quenching (ACQ). For example, PAH-based luminogens like pyrene and its derivatives emit deep blue emission with high quantum yields at low concentrations, which has limited its application as an efficient solid emitting material.[2,9]

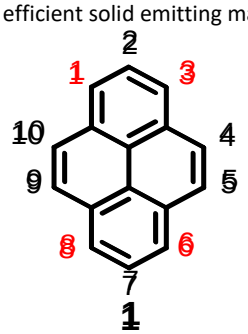

Figure 1. The molecular structure of pyrene **1**.

The intrinsic properties of pyrene alone do not make it a good candidate for light emitting devices, however, the ACQ effect of pyrene has been overcome by introducing bulky groups with long alkyl chains which enhances the fluorescence quantum efficiency in OLEDs and also reduces the aggregation of the final material.[2] For example, a 1,3,6,8 substituted pyrene based conjugated molecule such as 1,3,6,8-tetrakis(4-butoxyphenyl)pyrene exhibits an active emitting layer in simple solution-processed OLEDs producing deep blue emission (CIE = 0.15, 0.18) and maximum efficiencies and brightness levels of 2.56 cd A^{-1} and 5000 cdm^{-2}.[11]

Experimentally, the planar structure of pyrene prefers to adopt a close-packing form in the aggregation state. The π–π stacking

[a]*School of Materials and Energy, Guangdong University of Technology, Guangzhou 510006, P.R. China.E-mail: hyxhn@sina.com*
[b]*Chemical Research Division, Bangladesh Council of Scientific and Industrial Research (BCSIR), Dhanmondi, Dhaka-1205, Bangladesh.*
[c] *Department of hemistry & Biochemistry,, University of Hull, Cottingham Road, Hull, Yorkshire HU6 7RX, UK.*
†*This review is dedicated to Emeritus Professor Takehiko Yamato (Saga University, Japan) on the occasion of his 66th birthday.*

Please do not adjust margins

interaction prompts the formation of detrimental species as excimers, resulting in the observed ACQ effect. Pyrene-based highly efficient emitting materials can be obtained by introducing various substitutions at the 1-, 3-, 6-, and 8- positions of the pyrene core.[2] Generally, these four positions are significantly more active than the other positions (the 4-, 5-, 9-, and 10-positions or the 2- and 7-positions) and it is not easy to directly substitute at these latter positions versus the 1-, 3-, 6-, and 8-positions.[9] Theoretically, the energy of the 1-, 3-, 6-, and 8-positions are lower by 8.8 kcalmol^{-1} than the 2- and 7-positions, and the substitution order follows the trend 1->8->6->3-.[12] Pyrene can be easily modified at the 1-, 3-, 6- and 8-positions to form mono-, di-, tri- and tetra-substituted derivatives[13] in a manner that can hinder π–π interactions to effectively suppress the excimer formation.[14] The introduction of bulky groups at the 1-, 3-, 6- and 8-positions of pyrene lead to a shift in the main absorption and emission bands into the visible region due to the extension of the π-conjugation system. On the other hand, as the nodal plane of pyrene passes through its carbon atoms at the 2,7-positions in the highest occupied molecular orbital (HOMO) and lowest unoccupied molecular orbital (LUMO), substituents at these positions will interact weakly with the central core.[15]For example, the uridine ring exhibited a weak electronic interaction with the pyrene core when it was substituted at the 2-position instead of the 1-position.[16] Thus, our group has previously focused on synthetic methodologies for the functionalization of the pyrene core to suppress the ACQ effect based on its special electronic structure, and numerous novel synthetic routes for the functionalization of the pyrene core have been explored. Examples include *tert*-butylation, electrophilic substitution, formylation, halogenation, oxidation, and borylation. Moreover other research groups have also attempted to explore a wide variety of methods including physical, and engineering approaches and processes, but the results to-date are far from satisfactory.[17]

1.2. Pyrene-based aggregation-induced quenching luminogens

The design and synthesis of efficient, stable pyrene-based fluorescent materials has been an active topic in the area of organic light emitting diodes (OLEDs).[18,10b]However, the π-aggregates/excimers in concentrated solution and the solid state,[19] lead to the formation of π-aggregates/excimers and subsequent quenching of fluorescence with low photoluminescence (PL) quantum yields (Fig. 2).[20,21]As a result, much effort to improve the photophysical properties of pyrene has been conducted.[1a,22] Thus far, the pyrene derivatives that have been reported still present some degree of fluorescence quenching in the solid state.[11,6] Therefore, the preparation of compounds based on pyrene that emit efficiently in the solid state remains an attractive objective.

Research to modulate the photophysical properties of pyrenes to enhance fluorescence both in solid and (or) in thin film is currently being conducted.[23] Using synthetic methods for the functionalization of the pyrene core, 1-substituted, 1,3-di-substituted-, 2,7-di-subsituted-, 1,3,6,8-tetrakis-substituted-, 1,3,5,9-substituted-, 4,5,9,10-substituted-pyrenes have been explored. However, all of above-mentioned compounds are ACQ compounds, because of the low quantum yields in the solid (film) state compared to those in solution. For example, 1,3,6,8-tetraphenylpyrene (TPPY, Fig. 2) is highly fluorescent (Φ ca. 0.9) in solution and the organic light emitting field-effect transistor devices (OLEFET) based on TPPY have been shown to exhibit electroluminescence (EL) with an external quantum efficiency of only 0.5% due to aggregation.[24,6] Thus, conventional dyes suffering from the ACQ effect may not be suitable for constructing highly efficient non-doped OLEDs. However, materials with non-planar propeller shape molecular structures exhibiting aggregation-induced emission (AIE) characteristics may be an ideal choice for non-doped OLEDs.

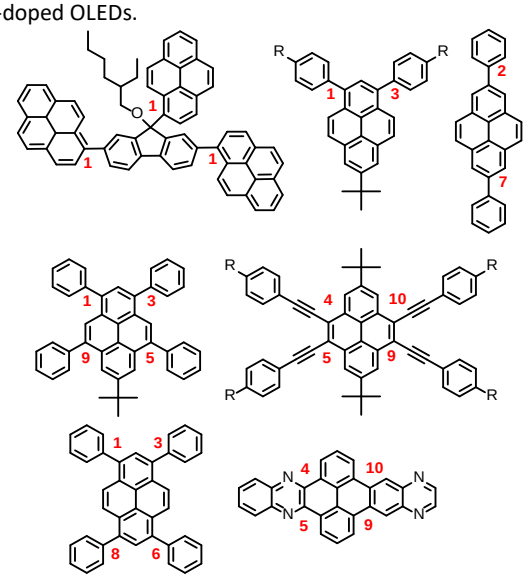

Figure 2. Chart of the molecular structures of pyrene-based blue emitters with the ACQ feature.[19,20]

1.3. Aggregation-induced emission

It is essential for organic luminescent materials to exhibit excellent optoelectronic properties (such as high fluorescence, good electronic/hole mobility etc.) for potential application in organic electronics, especially in solid state or the aggregated state. Tang et al. observed an abnormal photophysical phenomenon in hexaphenylsilole (HPS) in 2001 (Fig. 3), whereby weak emission was present in solution but enhanced emission in the solid state.[25] This phenomenon was the term as “aggregation-induced emission” (AIE), and the discovery of AIE solved the ACQ effect of traditional luminophores.[25] Recently, the AIE concept was widely accepted in the scientific community and more than 40000 papers on AIE research have been published, including on siloles,[26] tetraphenylethane (TPE),[27] 9,10-bis(p-dimethylaminostyryl)-anthracene (9,10-MADSA),[28] 1-cyano-*trans*-1,2-bis-(40-methyl biphenyl)ethylene (CN-MBE),[29] 2,5-diphenyl-1,4-distyryl-benzene (DPDSB) derivatives,[30] diphenyldibenzofulvene(DPDBF) derivatives,[31] conjugated polymers,[32] borondipyrromethene(BODIPY) derivatives,[33] triazoles,[34] and others.[35,36]

This journal is © The Royal Society of Chemistry 20xx

Please do not adjust margins

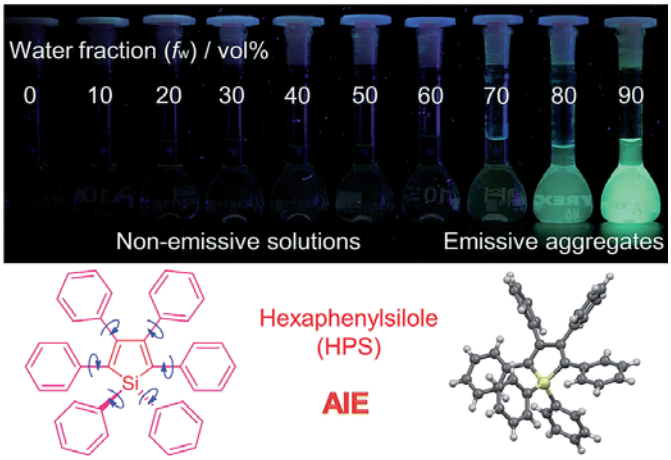

Figure 3. Fluorescence photographs of solutions and suspensions of hexaphenylsilole (HPS; 20 mM) in THF/water mixtures with different fractions of water. Reproduced from ref. 25d. Copyright (2014) Wiley-VCH.

Different hypotheses have been put forward for AIE mechanisms, such as *J*-aggregates, excited state intramolecular proton transfer (ESIPT), twisted intramolecular charge transfer (TICT) etc.[37] The restriction of intramolecular rotations/motion/vibrations (RIR/RIM/RIV) was widely accepted to explain the AIE mechanism. Take hexaphenylsilole (HPS) as an example, the six peripheral phenyl rotors were dynamically rotated relative to the central of silole, around the C-C or C-Si bond. The rotation of the aromatic rotors generally destroys the excitons in a non-radiative mode in the solution state; Upon aggregate formation, the emission intensity of AIEgens would be enhanced by the restricted intramolecular rotation (RIR), which blocks the non-radiative pathway for the excitons to decay with the activated radiative transition, thus the radiative decay of the excited state becomes dominant, rendering the luminogens emissive. As a consequence, the fluorescence quantum yields of siloles in aggregates is two orders of magnitude greater than in solution due to the restriction of intramolecular rotation (RIR) of the chromophoric compound.[25]

1.4 Jablonski diagram

A molecule in the excited state can decay in several ways as shown in the Jablonski diagram (Fig. 4).[38]Relaxation to the ground state from these excited states occurs by a number of mechanisms that are either radiation-less, in that no photons are emitted, or involve the emission of a photon. The most likely pathway by which a molecule relaxes back to its ground state is that which gives the shortest lifetime for the excited state, of the order of 10^{-15}s.[38].

By a combination of internal conversions and vibrational relaxations, a molecule in an excited electronic state may return to the ground electronic state without emitting a photon. A final form of radiation-less relaxation is an intersystem crossing in which a molecule in the ground vibrational energy level of an excited electronic state passes into a high vibrational energy level of a lower energy electronic energy state with a different spin state. For example, an intersystem crossing between a singlet excited state (S_1), and a triplet excited state (T_1). Fluorescence ($S_1 \rightarrow S_0 + h\upsilon$) occurs when a molecule in the lowest vibrational energy level of an excited electronic state returns to a lower energy electronic state by emitting a photon.

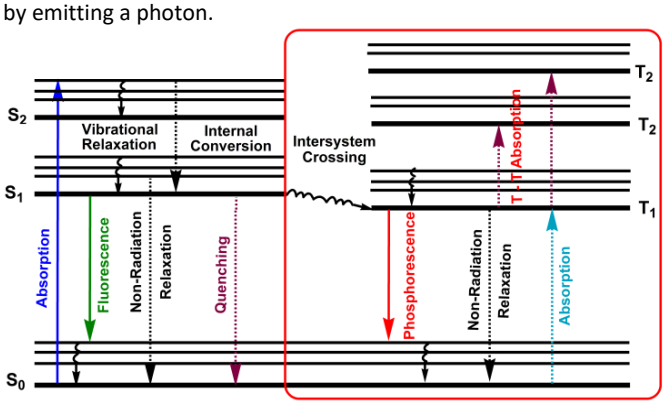

Figure 4. Jablonski diagram of the relevant photophysical processes in luminescence materials.

Phosphorescence ($T_1 \rightarrow S_0 + h\upsilon$) is most favourable for molecules that have $n \rightarrow \pi^*$ transitions, which have a higher probability for an intersystem crossing than do $\pi \rightarrow \pi^*$ transitions. Delayed fluorescence results from two intersystem crossings, first from the singlet to the triplet, and then back to the singlet state ($S_1 \rightarrow T_1 \rightarrow S_1 \rightarrow S_0 + h\upsilon$).

The intensity of fluorescence or phosphorescence *I*, is proportional to the amount of radiation from the excitation source that is absorbed and the quantum yield for fluorescence.

$I = k\,\Phi\,(A_O - A)$----------(i)

where *k* is a constant accounting for the efficiency of collecting and detecting the fluorescent emission. From Beer's law we know that

$A/A_O = 10^{-\varepsilon bc}$----------(ii)

where *c* is the concentration of the fluorescing species. Solving equation (ii) for *A* and substituting into equation (i) gives, after simplifying

$$I = k\,\Phi A_O(1-10^{-\varepsilon bc})\text{----------(iii)}$$

For low concentrations, where εbc is less than 0.01, this equation simplifies to

$I = 2.303\,k\Phi A_O\varepsilon bc$ ----------(iv)

According to the Jablonski diagram, upon aggregate formation, the emission of AIEgen is induced or revitalized by the specific effects of the RIR/RIM/RIV/ESIPT and the highly twisted molecular conformation that destroys the intermolecular π-π stacking interactions.[25,26] We will first carefully elaborate on the working principle of AIE and then demonstrate how to transform traditional ACQgens into new AIEgens, followed by the presentation of a series of new AIEgens derived from the RIR/RIM/RIV principle (Fig. 5). Finally, we will recap the research efforts devoted towards the exploration of technological applications of the new pyrene based AIEgens. To understand the mechanisms of AIE phenomena is of great importance to the quest for fundamental knowledge of photophysics, and just as crucial, it will guide our endeavors to design novel pyrene-based AIE luminogens, and to explore practical applications and technological innovations. Since the arrival of the AIE concept in 2001, researchers have shown persistent thirst for learning what are the real mechanistic causes for the AIE phenomena.[25,26]Herein, we will summarize new pyrene luminogens,

Please do not adjust margins

and more importantly, discuss a feasible method to realize the transformation of pyrene-based ACQ luminogens to AIE. The excellent optical properties of pyrene-based AIEgens for potential applications in organic semiconductor devices in biochemistry will be discussed, as well as recent developments in the area of chemisensors.

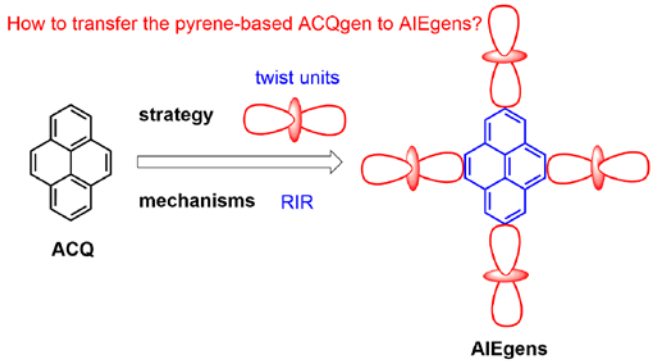

Figure 5. Schematic diagram of pyrene based AIEgens possessing bright emission.

2. Pyrene-based aggregation-induced emission luminogens

2.1 Pyrene core AIEgens

Since the emission of pyrene **1** is either weak or quenched in the solid state due to its planar structure with a large π-conjugation system, an effective approach to overcome this is the incorporation of bulky substituents or a spiro framework at the periphery of the pyrene core in order to inhibite the π–π interactions, leading to a highly emissive solid state. Arylsilyl substituted pyrene derivatives **2** and **3** were synthesized *via* Suzuki-Miyaura/Sonogashira-Hagihara cross-coupling reactions with corresponding with silyl-terminated group at the 1-, 3-, 6- and 8-positions. Triphenylsilylphenyl substituted pyrene **2** exhibited intense emission at 440 nm in the film with a high fluorescence quantum yield (Φ_f = 0.65); whereas triphenylsilylphenyl (ethynyl) substituted pyrene **3** showed an excimer emission with low $\Phi_f$both in THF solution (0.50) and as a film (0.16).[39]Despite the introduction of the bulky tetraphenylsilylethynyl groups in **3**, the pyrene moieties can clearly still interact in an orthogonal orientation. The DFT geometry optimization predicts that the incorporation of the coplanar phenylethynyl substituents in the structure of **3** results the Si atoms being 8.77 Å from the 1-, 3-, 6-, and 8- carbon atom positions, rather than 6.21 Å, as is the case in the structure predicted for **2** (Fig. 6).[39]

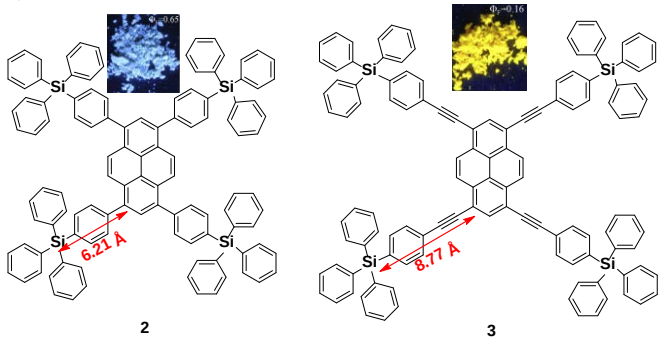

Figure 6. Structures of **2** and **3** calculated by DFT methods. Reproduced from ref.39.

The longer distance between the Si atoms and the 1-, 3-, 6-, and 8-positions on the outer perimeter of the pyrene π-system, probably enables significant π-π interaction to occur between neighboring pyrenes. Although the pyrene possesses a large π-conjugation planar structure, according to the RIR mechanism, it is possible to convert the pyrene into a highly-efficient pyrene-based AIEgen by introducing a twisted fragment, such as TPE or Triphenylethylene (TriPE) units etc. Zhao first introduced the TPE units at the pyrene core as peripheral ornaments affording TTPEPy **4** possessing a novel aggregation-induced enhanced emission (AIEE) effect (Fig. 7) It emitted sky-blue emission (483 nm) with efficient PL (Φ= 70%) in the solid state, and excellent thermal stability (Td = 485 °C).[40]The temperature-dependant PL spectrum was measured over the range 300K to 77K, and the fluorescence lifetime gradually lengthened from 0.25 ns at 300 K to finally 1.29 ns at 77 K. This was due to the intramolecular rotations of the TPE blades been greatly restricted at the cryogenic temperature and that the accompanying RIR process helped enhance the PL of TTPEPy **4** in the frozen solution.

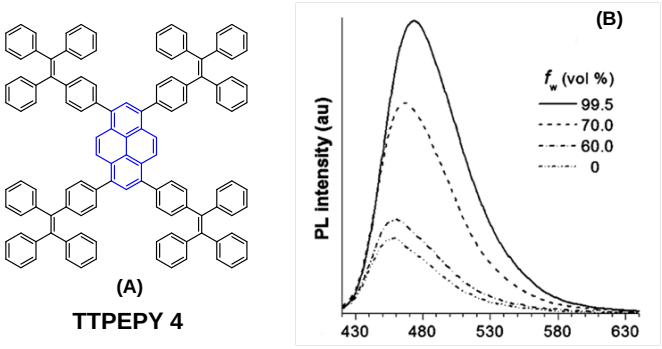

Figure 7. Structure of **4** and emission spectrum of **4** in THF with increasing percentage of water. Reproduced from ref. 12.

In addition, the construction of efficient non-OLEDs using TTPEPy a **4** as blue emitter, that display an excellent current efficiency (η_C), power efficiency (η_P) and maximum external quantum efficiency (η_{ext}) up to 12.3 cd A^{-1}, 7.5 lm W^{-1} and 4.95 %, respectively has been reported.[40] Furthermore, to investigate the relationship between the molecular conformation,the emission colour and the AIE properties, Li et al. designed and synthesized two pyrene-based luminogens, Py-4MethylTPE (**5**) and Py-4mTPE (**6**), see Fig. 8. The differing behaviour is due to the linkage mode at the *meta*-position which can twist the molecular structure and provide a new stereoelectronic effect (Fig. 8). Both compounds exhibit AIE and AEE effects, although they have minor differences in their structures, [41] for example the torsion angle of **5** between the pyrene core and the TPE periphery is larger than that of **6** due to the introduction of the methyl groups. On the other hand, use of *meta* linkages on the TPE moieties shortens the π-conjugation length in comparison with the para linkages and results in the increased in rotational barriers. The *meta* linkage is more effective at controlling the twisted conformation and generating enhanced molecular rotation. Given this, the compound **6** emitts a more blue emission at 445 nm compared with **5** which shows an emission

This journal is © The Royal Society of Chemistry 20xx

Please do not adjust margins

Please do not adjust margins

peak at 459 in the aggregation state. Importantly, when using compound **6** as emitter, the OLED device exhibits favourable EL properties with a lower turn-on voltage (3.5 V) and better OLED performance with values of $\eta_{C,max}$, ηP,max, and ηext,max at 4.02 cdA^{-1}, 3.08 ImW^{-1}, and 2.5 %, respectively.[41a]

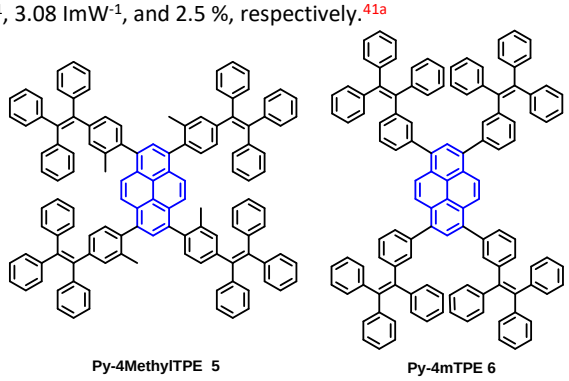

Figure 8. Structures of Py-4MethylTPE **5** and Py-4mTPE **6**.

It seems that it is an efficienct approach to achieve pyrene-based AIEgen through integrating pyrene with TPE units. Tao's groups has presented two (only one here?) pyrene-based fluorescent materials, namely 1-[4-(2,2-diphenylvinyl)phenyl]pyrene (PVPP**7**), which was synthesized via the Suzuki coupling reaction with TriPE units.[20b]

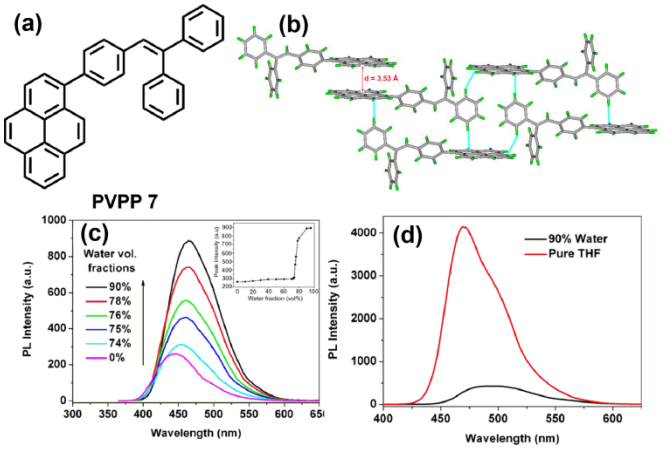

Figure 9. (a) Chemdraw representation of PVPP**7** and (b) molecular structure of PVPP**7**. (c) PL spectra of PVPP**7** in THF/water mixtures with different volume fractions of water. (d) PL spectra of TPVPP in pure THF and in a 90% water/THF mixture. Reproduced from ref. 20b.

Interesting, compound **7** shows a dramatic enhancement of fluorescence intensity with clear AIEE characteristics. Although the 1,3,6,8-tetrakis[4-(2,2-diphenylvinyl)phenyl]pyrene (TPVPP) with same triphenylethylene units, which is non-AIE-active compound. The single crystal X-ray diffraction analysis indicated that the two terminal phenyl rings in PVPP **7** are almost perpendicular with a twist angle of 89.3°, and that several intramolecular C-H$\cdots\pi$ interactions are present which can play a significant role in suppressing the fluorescence quenching of pyrene units in the solid state (Fig. 9d). The free twisting motion of the 1,1-diphenylvinyl motif is restricted by the intra- and intermolecular C-H$\cdots\pi$ hydrogen bonds. Thus, the non-radioactive decay channel is closed. More importantly, the molecular structure of PVPP**7** is significantly distorted and the twisted geometry can prevent the strong π–π interactions to produce intense fluorescence in the solid state. Li *et al* firstly introduced the twist terminal units at the 2,7-positions of pyrene to access the pyrene-based AIEgens **8**–**13** (Fig. 10). In this case, the AIE building blocks become more and more twisted, and large blue-shifted emission is achieved on moving from Py-2*m*TPE **9** (460 nm) to Py-2NTF **12** (456 nm) and to Py-2TF **13** (444 nm).[41b]

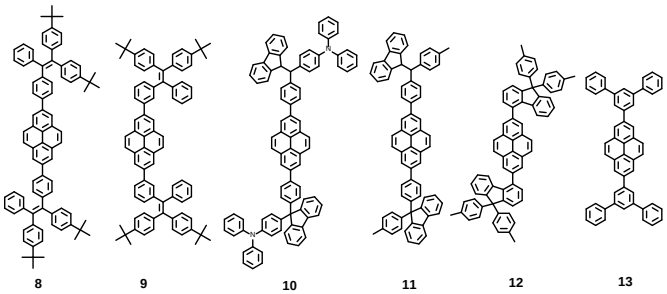

Figure 10. Structures of Py-2pTPE **8,** Py-2mTPE **9,** Py-2TP **10**, Py-2TF **11,** Py-2NTF **12** and to Py-2F **13**.

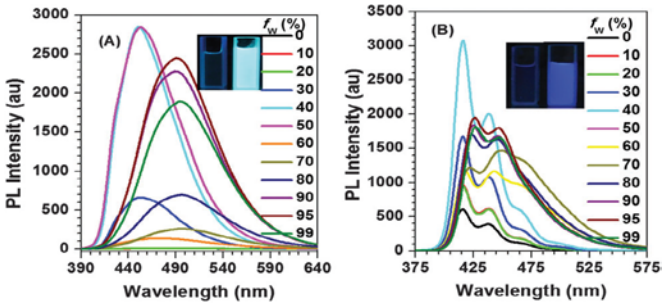

Figure 11. PL spectra in THF/H_2O mixtures with different water fractions:(A) Py-2*p*TPE **8**, concentration (mM): 12.0; excitation wavelength 330 nm; (B) Py-2TP **10**, concentration (mM): 14.0; excitation wavelength 300 nm. Inset: Photos of Py-2pTPE **8** and Py-2TP **10** in THF/H_2O mixtures (fw = 0 and 99%) taken under the illumination of a 365 nm UV lamp. Reproduced from ref. 41b.

Py-2NTF **12** exhibited a blue-shifted absorption compared to Py-2F **13**, owing to the weak conjugation at the 9,9´-positions in the fluorene (13 does not contain fluorine see need to be clearer here)as well as the severely twisted conformation of this linkage mode. There was little difference between Py-2NTF **12** and Py-2TF **11** in the UV absorption spectra due to the non-conjugated 9,9´-positions of fluorine??. In detail, for Py-2pTPE **8** and Py-2mTPE **9**, which consisted of typical AIE units of tetraphenylethene shows typical AIE characteristics (that show a non-emissive –in pure THF solution but a strong fluorescence in the aggregation state.).

Interestingly, for Py-2pTPE **8** (Fig. 11), as the water fraction was varied over the range 30% to 50%, it exhibited a deep blue emission which peaked at about 450 nm. The luminescence intensity increased gradually, and reached a maximum at 50% water fraction. However, when the water fraction increased to 60%, only very weak luminescence was observed and its emission peak was red-shifted to about 494 nm. This abnormal phenomenon originated from the transition of the crystalline state to an amorphous state.[41b]

More recently, the group of Tang reported a new strategy to achieve white-light emission from single tetraphenylethylene substituted pyrenes (TPE-Pys) **14**–**16** with aggregation-induced

Please do not adjust margins

Please do not adjust margins

emission (AIE) characteristics (Fig. 12).[42] These molecules exhibited tunable emission from blue (474 nm) to yellow (531 nm) both in solution and in the solid state. Specially, **14c** and **16** emitted a dual fluorescence at around 436 nm and 538 nm in a water fraction of 80% appears to result in a and a warm white light with a CIE of x=0.30,y= 0.41.[42]These compounds emit white-coloured fluorescence in THF/water mixtures. Indeed, these are rare examples of white-light emission achieved from a single AIE-active molecule *via* the control of its aggregated state emission by tuning the composition of the solvent mixture.

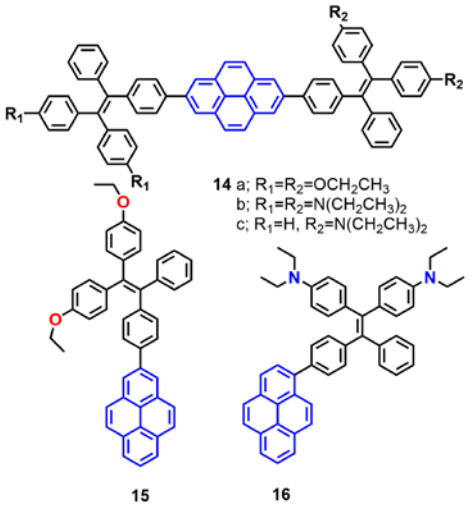

Figure 12. Structures of TPE-Pys**14**–**16**.

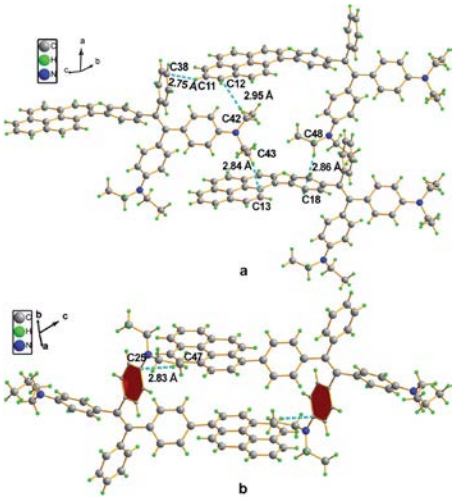

Figure 13. Single crystal structure of **16**: (a) face-to-face pattern of pyrene moieties separated by TPE units and (b) head-to-tail packing mode with multiple C–H···π interactions with a distance of 2.83Å. Reproduced from ref. 42.

A single crystal X-ray diffraction study indicated that compound **16** adopts a twisted conformation andrevealed that the torsion angle between the terminal pyrene ring and the benzene ring of the TPE is 48.6° (Fig. 13). The molecular motion of the TPE moiety is suppressed by multiple intramolecular C–H···π interactions with distances of 2.75–2.95 Å. The pyrene rings are arranged in a head-to-tail fashion and are separated by the TPE units at a large distance of 8.08 Å. This prevents their π–π stacking which would quench the light emission. Multiple C–H···π interactions are formed in the crystal lattice which effectively restrict the phenyl rings of TPE from undergoing intramolecular motions. The non-radiative decay pathways are blocked to allow **16** to emit intense light in the aggregated state. [42]

2.2. TPE-like Pyrene-based AIEgens

Tetraphenylethylene (TPE) has attracted much attention because it possesses advantages such as efficient solid-state emission, facile synthesis and ease of functionalization.[43,44] More importantly, TPE is a promising candidate to convert conventional ACQ chromophores into effective AIEgens with excellent photoluminescence properties.[45] Given their outstanding AIE properties, much effort has been devoted to developing TPE-like based AIEgens which are expected to have large π-conjugation as well as enhanced emission behaviour in solid state. The main approach to obtain efficient solid photoluminescence is to replace the phenyl rings of TPE by polycyclic aromatic hydrocarbons (PAHs) which introduce increased π-conjugation into the system. To date, several TPE-based AIEgens with notable solid-state emission have been developed.[46] Researchers have speculated whether a tetra(polycyclicaryl)ethene with excellent solid-state emission can be obtained by carefully selecting PAHs as substituent groups. These PAHs not only have an enlarged π-conjugated system but also have effective steric hindrance to restrict the formation of π-stacking.

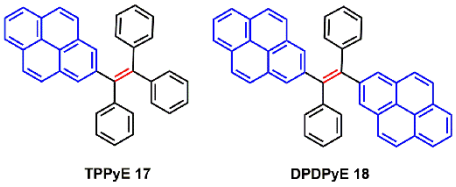

Figure 14. Structures of **17**,**18**.

To verify this assumption, scientists have utilized many PAHs such as pyrene, fluorene, naphthalene, biphenyl etc to assemble tetra(polycyclicaryl)ethene.[47]Zhao *et al*. reported two pyrene-substituted ethenes, namely TPPyE**17** and DPDPyE**18** (Fig. 14), where the phenyl ring of TPE was replaced by a pyrene ring. Unexpectedly, both the TPE-like pyrene-based dyes exhibited clear AIE features and were weak emitters in solution, but they became strong emitters when aggregated in the condensed phase.[46a] The crystal packing indicated that the intramolecular rotation was suppressed by π–π stacking and multiple C–H···π interactions. These structural features block the non-radiative energy decay channels, and allow for intense emission in the solid state.

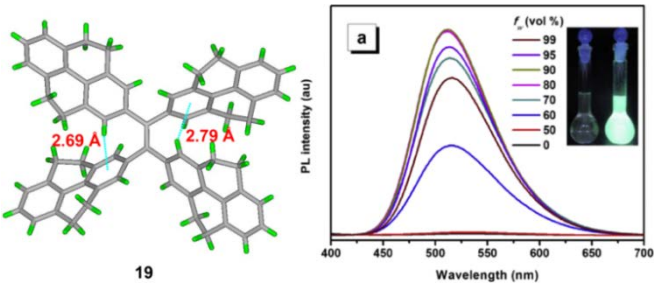

Figure 15. Crystal structure of **19** and PL spectrum of compound **19** in THF/water mixtures with different water fraction (fw). Inset: photos of compound **19** in THF/water mixtures (fw = 0 and 90%)

This journal is © The Royal Society of Chemistry 20xx

Please do not adjust margins

Please do not adjust margins

under UV lamp illumination. Excitation wavelength: 370 nm. Reproduced from ref. 47.

Furthermore, using TPPyE**17** and DPDPyE**18** as high-efficiency emitters, green OLEDs were fabricated with maximum luminance and power, current, and external quantum efficiencies of 49830 cd m^{-2} , 9.2 lm W^{-1} , 10.2 cd A^{-1} and 3.3% respectively. To investigate the effect of substituent size on molecular rotation, Ni *et al* reported tetrakis(4,5,9,10-tetrahydropyren-2-yl)ethene **19**, which exhibits clear AIE characteristics.[47] The fluorescence quantum yield of tetrakis(4,5,9,10-tetrahydropyren-2-yl)ethene **19** in a solid film is up to 74.1%. A crystal structure analysis indicates that there are no π-stacking interactions present (Fig. 15). This study reveals that when constructing aggregation-induced emission molecules using substituent groups with expanded π-conjugation, introduction of appropriate steric hindrance on the substituent groups can effectively restrict the formation of excimers. Meanwhile, hydrogen atoms from the ethylidene groups of compound **19** tend to interact with the π-cloud center of the closest two phenyl rings from the adjacent molecules and these multiple C–H···π interactions rigidify the molecular structure and restrict the rotation of **19**, thereby making a valuable contribution in avoiding the formation of excimers. Thus, compound **19** exhibited high emission in the solid state with a high quantum yield (74.1%) compared to that observed in THF solution (1.25%).[47]

On the other hand, it is an efficient approach to construct AIEgens by expanding the π-conjugation of ethene derivatives using pyrene units. Li *et al*. further published a series of efficient lTPE-like (is this supposed to say TPE-like) pyrene-based blue materials **20**–**25** with an AIE building block acting as the core and pyrene as a peripheral group. These compounds showed enhanced hole-transporting ability, achieving a good interaction between pyrene substituents (Fig. 16).[48]

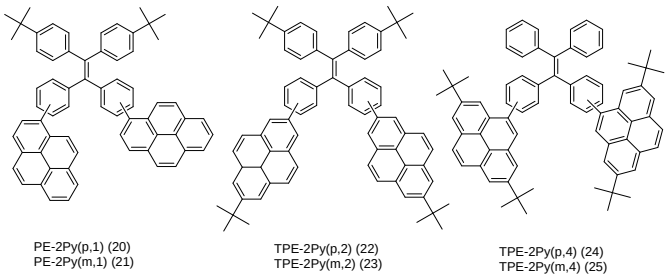

Figure. 16. Structures of **20**–**25**.

The effect of substituent position on the emission colour and electrocluminescence were investigated by modifying the linkage modes of TPE (*para* to *meta*-position) and pyrene units (1- to 2- to 4- position). All of these pyrene derivatives exhibited apparent AIE characteristics and comparable EL performances in their OLED devices. When the pyrene units were attached at the *meta*-position of TPE, the PL emissions were tuned to deep blue (452 nm) in the solid state,[48] with that at the pyrene 4-position producing a better deep blue emitter than the 1- or 2- substituted pyrenes. Using TPE-2Py(p,4) **24** as a hole-transporting material, the resulting blue OLED device exhibited excellent EL performance with a current efficiency and external quantum efficiency up to 4.66 cdA^{-1} and 2.79% respectively at the CIE coordinate of (0.16, 0.21).[48]

Furthermore, Yanget *et al* reported the highly efficient blue emitter TPE-4Py**26** with an AIE effect, which is achieved by a combination of twisted tetraphenylethene (TPE) core and planar pyrenes on the periphery.[49] Its EL efficiency was enhanced in doped OLEDs, at high doping concentration (50%), with a current efficiency up to 4.9 cdA^{-1} at 484 nm (Fig. 17). The twisted conformation of **26** led to weak conjugation as well as blue emission. Furthermore, the π–π stacking was effectively restricted, which resulted in an abnormal AIE effect. The optimized structure revealed a heavily twisted conformation with a torsion angle of about 50° for the TPE, while the dihedral angle between the pyrene and the adjacent phenyl ring was as wide as 60°.[49]

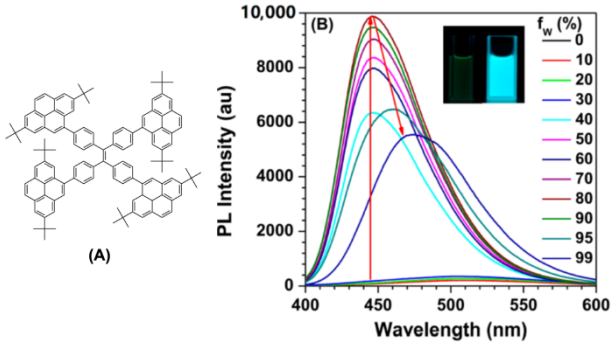

Figure 17. (**A**) Molecular structure of TPE-4Py **26**; (**B**) The PL spectra of TPE-4Py **26** in THF/H_2O mixtures with different water fractions. Concentration: 10 μM; excitation wavelength: 330 nm; inset: photographs of theTPE-4Py **26** in THF/H_2O mixtures (f_W = 0% and 90%) taken under the illumination of a 365 nm UV lamp. Reproduced from ref. 49.

2.3. Non-typical Pyrene based AIEgens

A study of vinylene-based materials revealed that the vinylene bond geometry plays an important role on the emission.[50] For example, the *cis*-isomer in poly(p-phenylenevinylene) (PPV) molecules generally possesses weak luminescence.[51]However, random placement of *cis*-olefin linkages along the PPV chain significantly increases the luminescence efficiency. For vinylene-based chromophores with an AIE or AIEE property, most tend to adopt the *trans*-isomer conformation.[51]According to the RIR mechanism, the C=C bond is used for constructing the AIE molecular?. For example, 1-[(9-anthracenyl)vinyl]pyrene (AVP) based AIEgens *trans*-AVP **27** and *cis*-AVP **28** are presented in Figure 18, and although the large planar structure of the pyrene and anthracene are both ACQ active, the anthracene ring was connected to a pyrene unit via a vinyl bridge and shows a clear AIEE characteristic with the two isomer conformations in the crystalline state.[52]

The quantum yield of *trans*-AVP **27** and *cis*-AVP **28** are 54.0% and 36.0% in the solid state *versus* in solution 15.0% and 17.0%, respectively. The interacting adjacent molecules in crystals of *trans*-AVP **27** adopt both edge-to-face and face-to-face arrangements. In contrast, in crystals of *cis*-AVP **28**, the adjacent molecules are inclined to adopt an edge-to-face arrangement and the molecular packing plays an important role in the solid emission efficiency.[52] Similarly, Li *et al* systematically investigated the substituent position and the vinylene bond geometry on the AIE features and the fluorescence solvatochromism. The structure of the (9-

Please do not adjust margins

Please do not adjust margins

Anthryl)vinyl(1-pyrenyl)vinylbenzene isomers **29**–**32** are presented in Figure 19.[53]

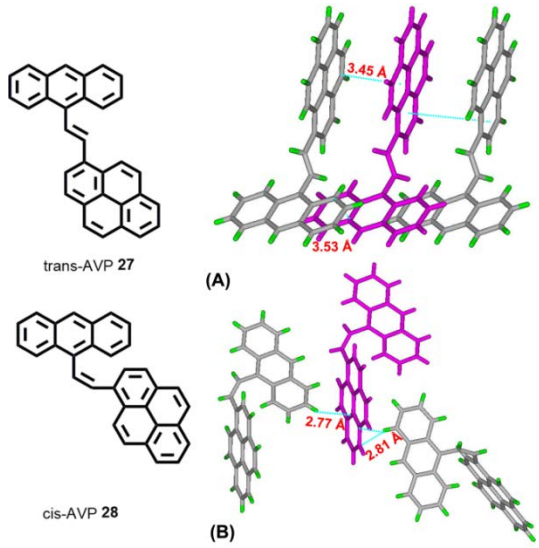

Figure 18. Structures of (A)*trans*-AVP **27** and (B)*cis*-AVP **28**, and their crystal packing.

Due to the differences in the molecular conformations, the series of compounds exhibit different fluorescence properties. For example, the *trans*,*trans*-1-(9-anthryl)vinyl-4-(1-pyrenyl)-vinylbenzene (*trans*,*trans*-1,4-AVPVB **31**), shows unusual AIE characteristics with fluorescence solvatochromism and emission shifts of over 80 nm, whilst *trans*,*trans*-1-(9-anthryl)vinyl-3-(1-pyrenyl)-vinylbenzene (*trans*,*trans*-1,3-AVPVB **30**) exhibited a weak solvatochromic effect due to the *meta*-substitution which emits most efficiently in solution. In addition, the *trans*,*trans*-1,2-AVPVB **29** and *trans*,*cis*-1,4-AVPVB **32** display moderate fluorescence and solvatochromism.

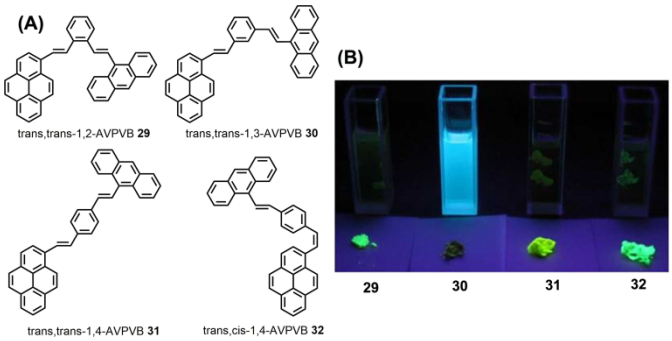

Figure 19. Structures and fluorescence images of the **29**–**32** in CH_2Cl_2 solution (upper) and as solids (lower) (from left to right) under illumination with a 365.0 nm UV lamp.

Theoretical calculations indicate that the fluorescence solvatochromism is related to the conformational change from the ground to the excited states due to the conjugate effect. An X-ray diffraction study revealed that the dihedral angle (53.98°) between the pyrenyl and the central benzene ring in *trans*,*cis*-1,4-AVPVB **32** is higher than that observed for *trans*,*trans*-1,4-AVPVB **31** (22.46°), which is due to the strong intramolecular C-H···π steric hindrance between the pyrenyl ring and its adjacent phenyl in *trans*,*cis*-1,4-AVPVB **32**. Therefore, the *trans*,*trans*-1,4-AVPVB **31** molecule is more planar and has better π-conjugation than does *trans*,*cis*-1,4-AVPVB **32**.[53]

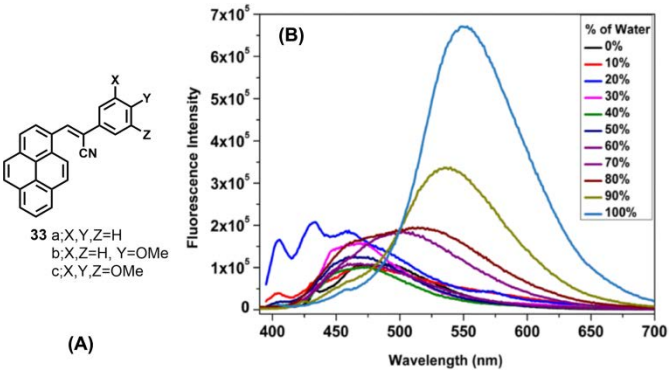

Figure 20. Structures of **33**.(a) Emission of **33c** in 1,4 dioxane/water system. Reproduced from ref. 54.

On the other hand, α-cyanostyrenes of type **33** bearing a pyrene scaffold are weakly emissive in solution but show broad red-shifted emission in water due to aggregation (Fig. 20).[54] mMethoxy substituted pyrenyl styrenes (**33b** and **33c**) exhibit a broad emission peak (~550-560 nm) with a shoulder peak (~460 nm) in polar acetonitrile. In the solid state, **33a** shows a clean emission spectra with maximum peak at ~510 nm, while **33b** and **33c** exhibit a noisy emission spectrum with bands at ~495 nm and at ~530-540 nm, respectively. The presence of the methoxy groups led to the formation of uniformly shaped aggregates and the resulting unique emission behaviour.[54]On the other hand, the emission of **33c** exhibited a bathochromic shift in different water fraction peaks (λ_{em} = 516 nm in fw = 60%, λ_{em} = 535 nm in fw = 90%,λ_{em} = 550 nm in fw = 100%),due to the formation of J-aggregates dominated by head to tail interactions.

2.4. Pyrene-based chalcone AIEgenyrene-based chalcone derivatives, formed by combining chalcone units with a pyrene core, exhibit special optoelectronic properties, due to a push-pull conjugation effect that improves the luminescent properties and redox activity, whilst the α,β-unsaturated ketone linkage enhances the non-linearity.[55,56]The molecular structure of such pyrenes consists of a donor with an electron-deficient keto vinyl (acceptor) linkage, which helps construct a D-π-A type conformation, which is responsible for the interesting AIEE/AIE features which enhance the luminescence properties of these materials. For instance, the four chalacone dyes **34**–**35** emitted yellow-green light in the solid state, and showed a large Stokes shifts *versus* their solution behaviour.[55]The fluorescence spectra of the methoxy-containing dyes **34a** and **35a** are found to be blue-shifted by 10 nm relative to the parent ones and the beneficial effect of the methoxy function on the degree of aggregation was observed. Quantum yields of **34b** (16%) and **35b** (19%) were found to be higher in the solid state than in solution, which thus showed a clear AIEE characteristic.

The X-ray crystal structure of **35b** revealed stacks of head-to-head oriented chromophores (Fig. 21).[55] The case of the dye **35a** is differentfor two reasons, firstly, it forms dimers in which the π -

This journal is © The Royal Society of Chemistry 20xx

Please do not adjust margins

systems of the pyrene styrenyl units in adjacent molecules are parallel, oriented head-to-head, and have no π -overlap.

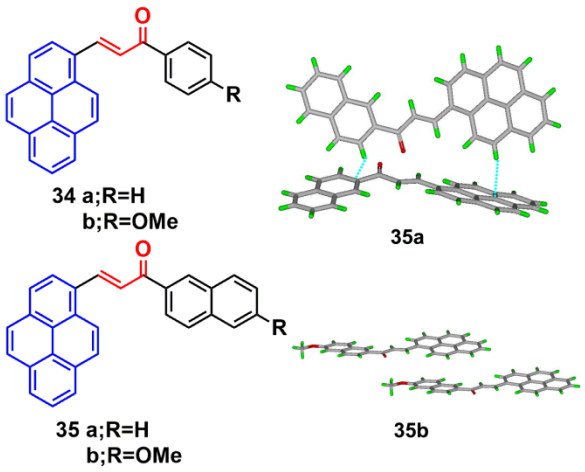

Figure 21. Crystal packing diagram of **34**, **35** illustrating π-π stacking interactions. Reproduced from ref. 55.

Secondly, the pyrene moieties of adjacent dimers of the former type overlap in an antiparallel fashion with an interplanar distance of 3.489 Å. The X-ray structure of **35a** reveals the presence of H-like aggregates, which may explain the quenching of the photoluminescence in these systems as compared to their CH_2Cl_2 solutions (Fig. 21). The X-ray structure of **35b** indicates a J-type aggregation that is not detrimental to the solid-state emission.[55]

On the other hand, pyrene-based chalcone materials containing heterocyclic five membered rings (**36**–**37**) were synthesized by a Claisen-Schmidt condensation, and exhibit an aggregation-induced enhanced emission (AIEE) with dual emissive characteristics in solution as well as in the solid.

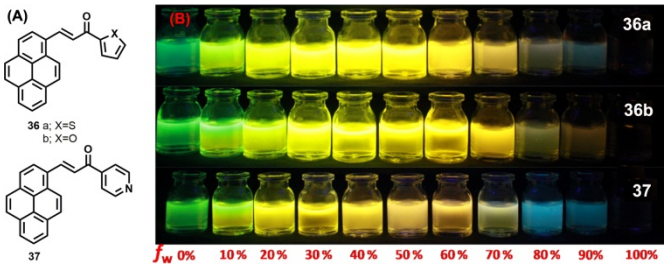

Figure 22. Photograph on AIEE property of PCT, PCF and PCP in THF/water mixture different water fractions (Fw = 0–100%) under illumination of long UV light (365 nm). Reproduced from ref. 56.

Specifically, the compounds **36**–**37** showed a large tunable colour emission from green to orange emission depending on the water fraction in THF/H_2O mixture (Fig. 22).[56]In the solid state, three compounds underwent a red shift of 77 nm, 82 nm and 81 nm of **36a** (PCT), **36b**(PCF) and **37** (PCP) compared to their solution state, respectively. Among them, **36b** (488 nm) and **37** (486 nm) displayed a small red-shifted emission wavelength (λ_{max}) than **36a** (481 nm) in solution.- makes no sense This may be attributed to greater intermolecular interactions in solid state of **36b** which occur because of the presence of the more electronegative and efficient electron accepting nature of the oxygen in furan. In the solid state emission spectra, **36a** exhibits a maximum emission at 558 nm whereas **36b** and **37** display maxima at 569 and 568 nm, respectively.[56] Compound **36b** exhibited greater fluorescence than **36a** and **37**, which is attributed to intermolecular interactions of the pyrene unit, namely π-π stacking and a J-aggregation arrangement.. Indeed, compound **36a** (PCT) afforded a good emission quantum yield of 0.74, whereas for **36b**(PCF) and **37** (PCP) the quantum yields were 0.68 and 0.53 respectively.[56]

2.5 Pyrene based AIE active Schiff base molecules

Many scientists are attempting to use the AIE activity of pyrene derivatives to sense molecules by using push-pull or on-off procedures. Schiff base AIE systems have been identified on the basis of intensity turn-on at a specific wavelength.[57] novel pyrene-based Schiff base derivative **38** was synthesized *via* a condensation reaction and utilized as a turn-on fluorescence sensors towards Cu^{2+} and showed AIE activity in CH_3CN and water mixture up to 80% (Fig. 23).[58]The PL intensity of **38** was enhanced ca. 630-fold (Φ_f = 0.567 in CH_3CN:H_2O = 20:80) by increasing the water fraction of H_2O from 0% to 90% and with a red-shift from 455 to 471nm. The mechanism possibly arises from restriction of intramolecular rotation (RIR). Since, the single bond rotation is mainly responsible for the dominant non-radiative decay, the RIR effect might be the cause for the AIE nature of **38**. The hydrogen-bond formation, suppression of the PET process and suppression of charge transfer (CT) or even intramolecular charge transfer (ICT) are other mechanistic approaches for this category of AIEgens.[58] However, the PL spectra for **38** suggested that the red shift on aggregation probably originated from the suppression of the twisted intramolecular charge transfer (TICT). Various molecules act as turn-on sensors for a variety of cations and anions based on photo-induced electron transfer (PET), internal charge transfer (ICT), chelation enhanced fluorescence (CHEF) and deprotonation mechanisms.[59]

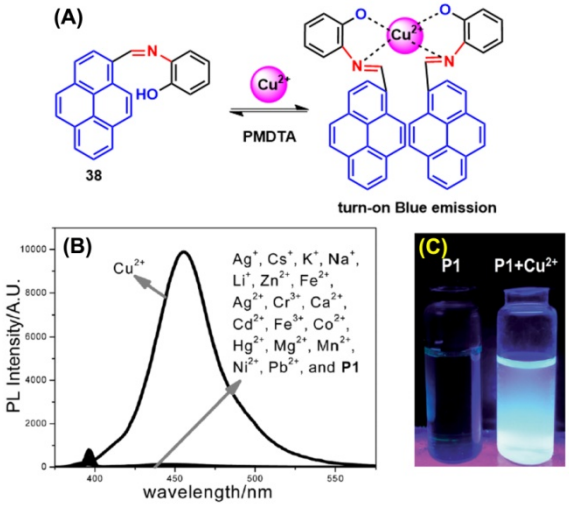

Figure 23. (A) Possible proposed binding mechanism of **38** towards Cu^{2+} ion. (B) Fluorescence emission spectra of compound **38** (10μM) upon addition of various metal ions. (C) Photographs of **38** and **38** + Cu^{2+} visualized under UV-light irradiations. Reproduced from ref. 58.

The photophysical properties of **39** revealed that the fluorescence of this molecule is completely quenched due to photo-

Please do not adjust margins

induced electron transfer (PET) processes in solution. The fluorescence intensity remains unchanged over the water fraction range o% to 70%. On further addition of water up to 90%, the emission intensity was enhanced with a red shift (25 nm) from 440 to 465 nm and with a concomitant increase in fluorescence lifetime.[60] This clearly signifies that this molecule exhibited an aggregation-induced emission (AIE) property.

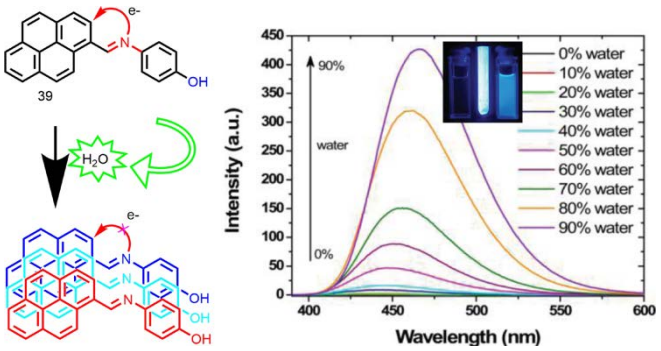

Figure 24.(A) **39** in THF and (B) **39** in THF/water mixture. Photographs taken under illumination of a UV lamp. (C) Emission spectrum of **39** in THF with increasing percentage of water. Reproduced from ref.60.

The AIE behaviour of **39** in the excited state was further investigated by the time-correlated single-photon counting (TCSPC) technique and the observed longer fluorescence lifetime is due to suppression of the PET process caused by aggregation of the **39** molecules.[60] Thus, the mechanism of AIE for this molecule is suppression of photo-induced electron transfer (PET) due to hydrogen bonding interactions of the imine donor with water.

Tunable pyrene based benzohydrazonate molecules of type **40** exhibit drastic aggregation-induced colour changes ($\Delta\lambda_{em,max}$ ~130 nm) with high solid-state quantum yields (~54.5%). The exciting switch behaviour is triggered by intermolecular hydrogen-bonding via the carbohydrozone bridge, which leads to stop the molecular conformations? (Fig. 25).[61] Upon increasing the amount of water in the DMF solution, the absorption did not significantly change until the water fraction reach 90% for (R=H) and 80% for (R=Cl, OMe), whereupon aggregation was initiated. The solid compounds **40** (R=Cl, OMe) revealed red-shifts of 54 nm and 42 nm compared to the spectra of the monomer state. – solid v monomer??

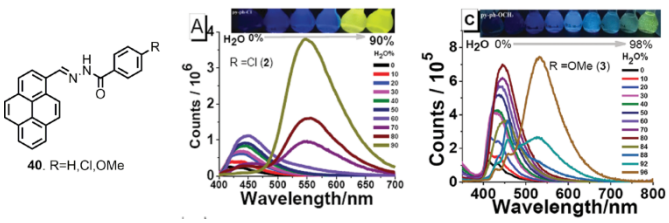

Figure 25. Structures and PL spectra of **40** in DMF/H_2O mixtures with different volume fractions of H_2O. Inset: Emission colour change from blue to yellow in aqueous DMF with f_w = 0–90% under 365 nm UV light. Reproduced from ref. 61.

Furthermore, compound **40** exhibited mechanochromic properties upon exogenic action. The blue-emitting pristine solids were converted to yellowish green emitting solids and the emission peaks exhibited varying degrees of red-shift. The pyrenyl-substituted acylhydrazone **41** derivative also exhibited favourable multiple luminescent switching mechano-fluorochromic behaviour. In particular, fluorescence colour changes visible by the naked eye, as well as emission that could be reversibly switched between a blue and a green colour as shown in Fig. 26.[62] By contrast, xerogel **41** obtained from DMSO revealed mechanofluorochromic behaviour, with the maximum emission peak shifted from 458 nm to 514 nm upon grinding. However, for 41 precipitated from THF, no mechanofluorochromic behaviour was observed. The different luminescent properties of **41** are attributed to the switch of the self-assembled structures via intermolecular hydrogen bonding which impacted on the translational and rotational motion of molecules, and thus the conformational flexibility of the pyrenyl moieties was restricted.[62]

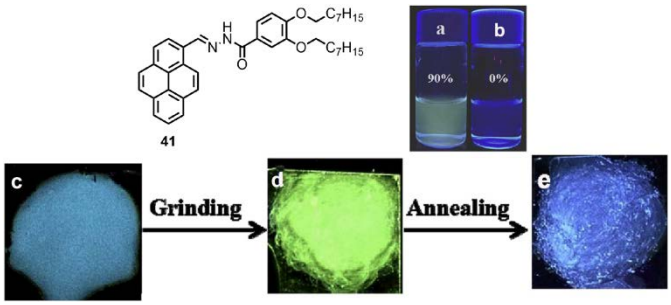

Figure 26. Emission spectra of **41** in 90 % of water (a) and THF (b). Photographs of emitting samples upon 365 nm UV illumination (c) xerogel **41**, (d) ground xerogel and (e) after annealing treatment . Reproduced from ref.62.

Two novel pyrene containing monomeric and dimeric Schiff base derivatives **42** and **43** were reported to show AIEE activity in DMSO upon addition of H_2O over the range 0% to 90% (Fig. 27).[63]

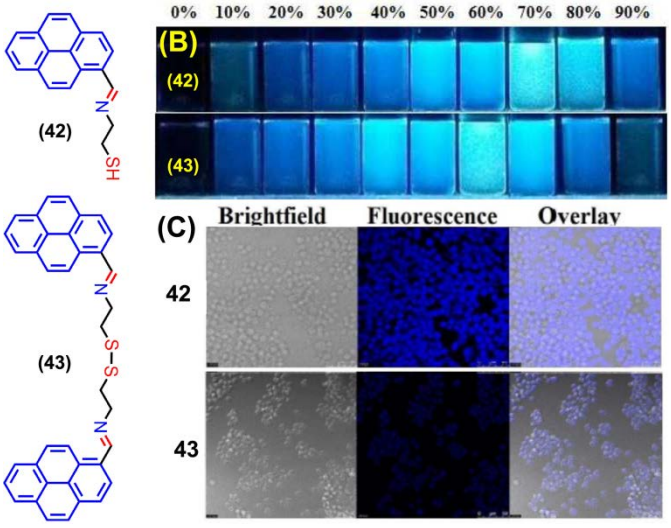

Figure 27. (A) – no A above! The structures of **42** and **43, (B)** photograph of the aggregation induced emission of **42** and **43** visualized under UV-irradiation (l = 365 nm). (C) Fluorescence

This journal is © The Royal Society of Chemistry 20xx

Please do not adjust margins

images of Raw264.7 cells treated with **42** and **43** at 12 hours. Reproduced from ref. 63.

Both **42** and **43** were also good sensors for trivalent metal ions (Fe^{3+}, Cr^{3+} and Al^{3+}) in living cells, for example, when Raw264.7 cells were incubated with **42**/**43** (10 mM in DMSO), no fluorescence was observed over 30 minutes. However, bright/dismal? blue fluorescence images were observed for the Raw264.7 cells after 12 hours due to intracellular H_2O induced aggregation. The bright cell image of **42** at 12 hours is due to the greater intracellular penetration of the free thiol unit, which is superior to the disulphide containing **43**.[63]Both **42** and **43** showed ''off–on'' sensing at highly acidic pH values (1–3)and were employed for live cell applications.[63]

2.6 ESIPT based AIEgens

Excited-state intramolecular proton-transfer (ESIPT) compounds have attracted attention due to their interesting and quite unique emission properties. Essentially by introducing aggregation-induced emission (AIE) phenomenon and excimer formation ability into molecular systems has provided the scope for dual emission. By contrast, ESIPT coupled-AIE phenomenon operate as an additional handle to adjust the emission wavelength of the corresponding emission peak by varying the solvent polarity.

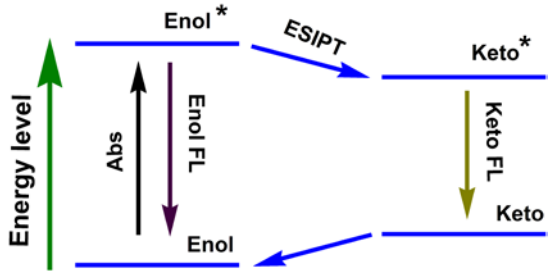

Figure 28. Four level schematic diagram of ESIPT.

The development of ESIPT molecules as probes is rapidly growing given the recent interest in their photophysical properties, such as unusually large Stokes shifts and outstanding environment-sensitivity that can readily be monitored by spectral changes.[64] It should ne noted that ESIPT molecules exist exclusively in an enolic form (E) in the ground state. Upon photoexcitation, extremely fast tautomerism from the excited enolic (E*) to the excited keto (K*) form occurs on a sub-picosecond time scale. After decay of K* to the ground state, the K form transforms to the initial E form through reverse proton transfer mediated by intramolecular hydrogen bonds (Fig. 28).The different species between absorbing and emitting in the intrinsic four-level photocycle (E-E*-K*-K) offer a high probability to address the disadvantage of fluorescence concentration quenching that is suffered by almost all of the currently available luminescent probes. On the other hand, ESIPT involves a proton-transfer process that is easily affected by changes in the surrounding conditions, leading to sensitive spectral responses. A single and broad emission peak because of a complete ESIPT is observed in polar solvents, while in non-polar solvents, conversion of the enol into the keto form is incomplete. The *J*-type aggregate effects may block the molecular motion and facilitate the ESIPT emission in the solid state / aggregated state.

Samanta *et al*. designed a simple AIE-ESIPT coupled organic molecule bearing a suitable fluorophore for achieving tuneable white light emission.[65] The designed molecule **44** was found to be very weakly emissive in pure methanol, but this was enhanced in methanol-water mixtures with large water contents (Fig. 29).

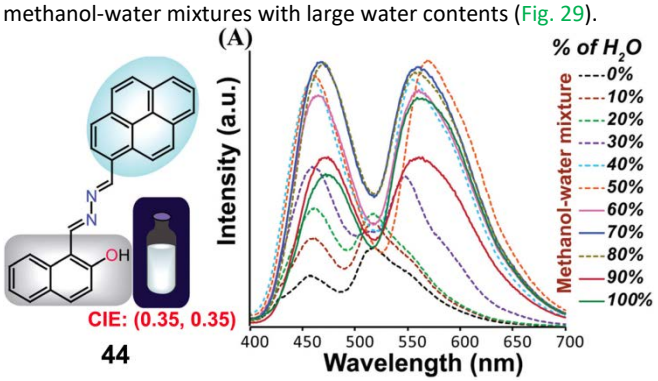

Figure 29. Structure of **44** and fluorescence spectra (10 mM) upon a change in the water fraction of a methanol–water mixed solvent; λ_{ex} = 380 nm;. Reproduced from ref. 65.

A pyrene based fluorescent probe, 3-methoxy-2-((pyren-2ylimino) methyl)phenol **45** (Fig. 30), was found to exhibit high sensitivity and selectivity toward Al^{3+} over other relevant metal ions and also displayed novel aggregation-induced emission enhancement (AIEE) characteristics in its aggregated/solid state.[66] This material could sense Al^{3+} in a 1:1 mode by signaling a significant fluorescence enhancement with a turn-on ratio of over ~200-fold sensor complex formation, and excess addition of Al^{3+} dramatically enhanced the fluorescence intensity over manifold through aggregation. The origin of such an AIEE phenomena for **45** was due to the single bond rotation, which is mainly responsible for the dominant non-radiative decay.[66] Thus , the RIR of **45** plays a crucial role in the AIEE characteristics as well as the PET off in the solid state. The same group also reported the AIEE materials **46** (Fig. 30), which can sense 2,4,6-trinitrophenol (TNP) by PET off and exhibit AIE in the aggregation state.[67]

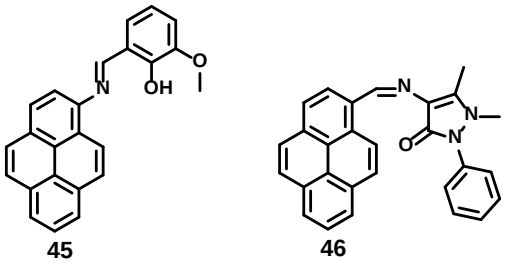

Figure 30. Structures of **45** and **46**.

2.7 Non-typical Pyrene based AIEgens: modification at the K-region

The pyrenoimidazoles **49** and **50** are weakly fluorescent in solution and their AIE behaviour has been studied in THF–water mixtures with different water content.[68] The poor fluorescence of pyrenoimidazoles **49** and **50** in THF was enhanced in aggregated suspension (95% water fraction) by 38 and 9-fold, respectively (Fig. 31). The pristine forms of pyrenoimidazole **49** and **50** absorb at 417 nm and 427 nm respectively, which upon grinding, exhibit

Please do not adjust margins

bathochromic shifts and absorb at 446 nm and 437 nm, respectively. RIR and XRD studies revealed that a transformation of the twisted crystalline state to the planar amorphous state.[68]

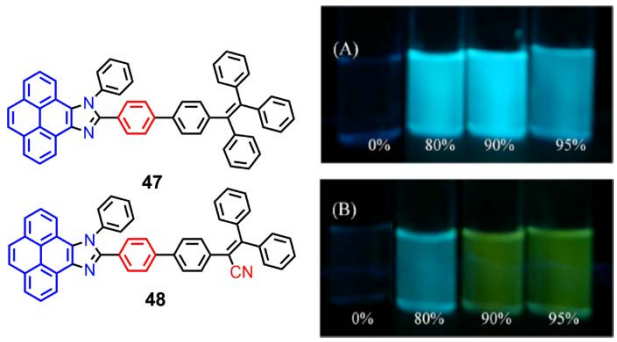

Figure 31. Photographs of **49** (upper) (A) and **50** (lower) in THF–water mixtures with different water fractions (10 mM) under 365 nm UV illumination. Reproduced from ref. 68.

The pyrene-imidazole-based structural isomers, axis symmetric *syn*-PyDTI **49** and centrosymmetric *anti*-PyDTI **50**, are non-emissive in THF but exhibited intense emission in their aggregate states. Crystalline *syn*-PyDTI **49** exhibited a 2-fold higher quantum efficiency than *anti*-PyDTI **50**, and displayed a much better performance in OLEDs with a $\eta_{C.max}$ of 11.4 cd A^{-1} (8.8 cd A^{-1} for **50**).[69]

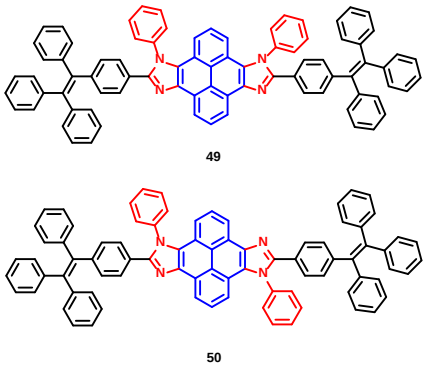

Figure 32. (A, C) Structures of syn-PyDTI **49** and anti-PyDTI **50**. (B, D) Unit cell structure top views of crystalline *syn*- and *anti*-PyDTI. Where? Reproduced from ref.69.

Comparing the crystal emissions revealed a red-shift for the *anti*-isomer **50**; that is, the *syn*-PyDTI **49** crystal exhibited an emission peak at 465 nm, whereas the *anti*-isomer **50** crystal displayed an emission peak at 507 nm. High-quality single crystals of *syn*- and *anti*-PyDTI emit blue and green respectively under UV light. The blue-shift observed for*syn*-PyDTI **49** was probably associated with the formation of dimers, which resulted in a flexible geometry and a decreased conjugation length (Fig. 32).[69] These observations reveal the dependence of molecular excited state properties on distinct structural symmetries. In recent years, pyrene-based, mechanochromism (MC)-active materials have been reported to have attractive excimer fluorescence in the solid state, which is in contrast to the frequently encountered ACQ phenomena in planar luminogens and offers the possibility to discover ML luminogens with planar structures.[70,71]

An outstanding feature associated with pyrene is its facile and varied structural modification.: In addition to its four main points of reactivity, i.e., the 1-, 3-, 6- and 8-positions, recent studies have revealed that the non-typical K-region (4-, 5-, 9-, and 10-positions) are also available for further modification.[2,9,72]In contrast to these recent advances at the 1-, 3-, 6,- and 8-positions, pyrene derivatives substituted at the 4-, 5-, 9-, and 10-positions (K-region) have been employed predominantly as synthetic intermediates for fused π-systems.[73] However, only a few studies have examined the effects of substitution at the 4-, 5-, 9-, and 10- position on the photophysical behaviour of pyrenes.[74]

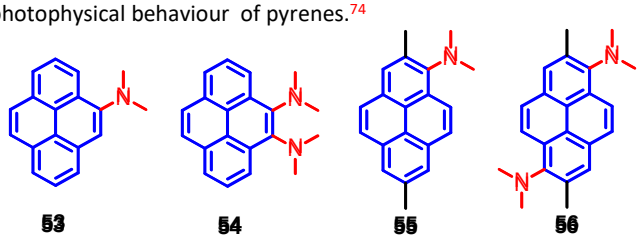

Figure 33. Structures of **53**–**56**.

A new design strategy was introduced by the Sasaki group in order to achieve AIE emission in pyrene chromophores. This was accomplished by introducing *N*,*N*-dimethylamine substituents at the K-region 4,5-positions of pyrene, , and these are likely to stabilize the minimum energy conical intersection (MECI).[75] Four pyrene derivatives, which contain highly twisted *N*,*N*-dimethylamino groups at the 4- (4-Py), 4,5- (4,5-Py), 1- (1-Py), or 1,6-positions (1,6-Py) are **53**–**56** (Fig. 33). The non-radiative transitions of 4,5-Py **54** are highly efficient (k_{nr} = 57.1 × 107 s^{-1}), so that its fluorescence quantum yield in acetonitrile decreases to Φ=0.04.[75] The solid-state fluorescence of 4,5-Py **54** is also efficient (Φ=0.49). By contrast, 1,6-Py **56** features strong fluorescence (Φ=0.48) in solution with a slow non-radiative transition (k_{nr} = 11.0 × 107 s^{-1}) that is subject to severe quenching (Φ = 0.03) in the solid state. The introduction of strongly twisted *N*,*N*-dimethylamines at the 1- and 1,6-positions resulted in intense fluorescence in solution. These differences are attributed mainly to non-radiative transitions. A comparison of the k_{nr} value of 4,5-Py **54** with its fluorescence energetics implies the involvement of a special pathway, e.g., a non-adiabatic relaxation via MECI, for efficient internal conversions.[75] The other derivatives **53** and **55** did not show noticeable emission changes in solution or the solid state, although they have AIE activity. The presence of highly twisted *N*,*N*-dialkylamino groups, especially at the 4,5-position, induces fast non-radiative transitions both in polar and non-polar solvents, resulting in faint fluorescence in solution.[75]

This journal is © The Royal Society of Chemistry 20xx

Please do not adjust margins

Please do not adjust margins

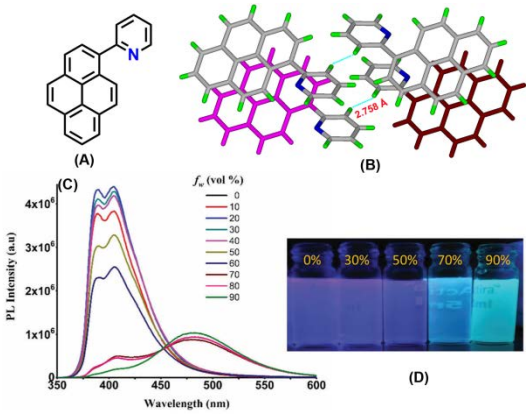

Figure 34. Emission spectra of **57** in different fractions of water in methanol and strong π–π interaction between the centroids of the two pyrene rings in the solid state. Reproduced from ref. 76.

Interestingly, a pyridine unit was introduced at the 1-position of pyrene, affording 2-(pyren-1-yl)pyridine **57** (Fig. 34).[76]This compound exhibits a typical AIEE feature, and mechanisms were proposed by RIR, whilst the crystal structure of **57** revealed the presence of a C-H···π interaction at 2.75 Å between two of the pyridine rings which blocks the rotation of the pyridine ring in the solid state (Fig. 34). Furthermore strong π–π interactions were observed in the range of 3.53–3.59 Å. Such short contacts would suppress the restriction of movement of the pyridine group in the solid state, and block the non-radiative pathways and open up new radiative pathways on progressive addition of water. On the other hand, the face to face π–π interaction also caused an excimer emission in the aggregation state or in the crystal state.

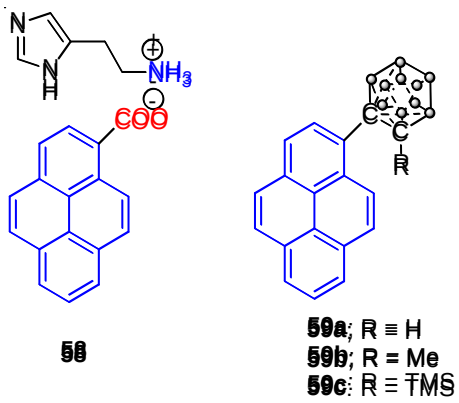

Figure 35. Structure of **58**–**59**.

Interestingly, Dastidar *et al* first observed the AIE phenomenon in organic salts. The primary ammonium salts of the pyrene-based carboxylic acid and histamine **58** (Fig. 35) exhibited an enhanced fluorescence in the solid state. The N acceptor and N-H donor of the imidazole moiety form a 3D hydrogen bonding network thereby imposed RIR in the solid state, and triggering AIE activity in the pyrene salt **58**.[77] The pyrene-substituted *o*-carborane dyads **59** (Fig. 35) were synthesized via the insertion reaction between decaborane and 1-ethynylpyrene in the presence of a Lewis base by using the Sonogashira−Hagihara coupling reaction. *O*-carborane dyads emits extremely bright light in the solid state (Φ_{PL}>0.99).[78]

2.8 Pyrene-based hexaphenylbenzene -like AIEgens

As above-mentioned, the steric interaction play a important role to effect the molecular configuration, as well as luminescence behavior. For example, the propeller-shaped hexaphenylbenzene (HPB), consist of six rotatable peripheral phneyl unitswith respect to the central benzene ring,shows an AEE character.[79] Following this in mind, new Pyrene-based hexaphenylbenzene-like AIEgens were explored as shown in Figure 36. Two phenyl units were replaced by pyrene ring, both*anti*-**60** and *syn*-**60** present novel AIEE characteristics with a multiple photoluminescence, including monomer, excimer and CT emission. The multipleemission mechanismsoriginated from the different spatial arrangements, due to the presence of large planar structure pyrene unit.[80]

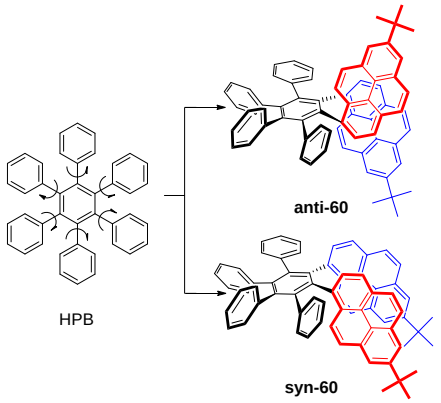

Figure 36. The structure of HPB and the pyrene-based hexaphenylbenzene -like AIEgens **60**.

3.0 Possible applications of pyrene-based AIE/AIEgens

"Touch a stone and turn it into gold": pyrene, a dim luminogen in solution, is possible to twist into a bright emitter as a solid by decorating it with suitable groups at different active positions. Solid-state fluorescent organic materials are essential components in optoelectronic devices, such as organic light-emitting diodes, solid-state lasers fluorescent, sensors, organic solar cells (OSCs).[8] However, the emission of most fluorescent organic molecules is effectively suppressed in the solid state, due to aggregation of the planar π-conjugation systems based on π-π interactions or the formation of excimers.[7] As a result, there has been considerable interest in preparing pyrene-based AIEgens which retain their photophysical properties in the solid state. Pyrene containing probes are very topical and remain of widespread interest because of their fast response via PET and excimer/exciplex formation towards specific species of interest.[81]

3.1 Organic light emitting diode (OLED)

Pyrene is well known as a good deep blue emitter and is often utilized to construct blue luminogens.[22a,82] An organic light emitting diode (OLED), also termed organic electro luminescent device (OELD), is a light-emitting diode (LED) whose emissive electroluminescent layer is composed of organic film. This layer of organic semiconductor material is formed between two electrodes, where at least one of the electrodes is transparent. The OLED materials as a flat-panel display, has many unique advantages, such as low driving voltage, high efficiency, excellent flexibility, vivid

Please do not adjust margins

colour, wide viewing angle. As a consequence, this technology has been used successfully for solid-state lighting applications. Pyrene is a promising chromophore with a high fluorescent quantum yield, and has attracted considerable interest in the design of small organic molecules for different applications including OLEDs[83]and organic field effect transistors (OFETs).[70,84] For example, the optimization of non-doped organic light-emitting diodes (OLEDs) using of pyrene-based 2,7-TPE substituted AIEgens led to emitters that displayed sky-blue light at 492 nm at a low turn-on voltage (3.1 V) with maximum luminance of 15750 cd m^{-2}, current efficiency of 7.34 cd A^{-1} and with low efficiency roll-off.[85]

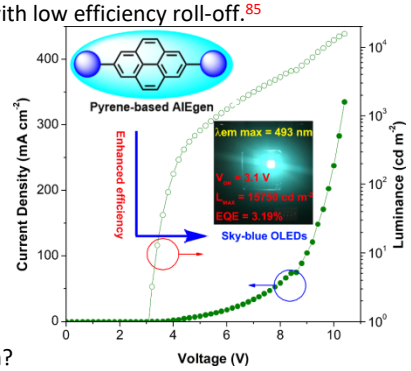

Caption?

Figure 37.
Reproduced from ref.85.

N,*N*-Di-*p*-methoxyphenylamine-substituted pyrenes have been successfully used as a hole transporting materials for perovskite based solar cells with high efficiency.[86] Since pyrene has extensive π-electron delocalization, it is a fascinating core for developing fluorescent π-conjugated light-emitting monomers substituted by a variety of functionalized groups or can be deployed themselves as substituents and introduced into others molecules to afford blue EL.

Advantages of pyrene **1** include is its excellent thermal and chemical stability, but it is not a good candidate for light emitting devices alone, due to its excimer emission tendency which lower the fluorescence efficiency.[10] However, this limitation has been overcome by introducing bulky groups with long alkyl chains which enhances the fluorescence quantum efficiency in OLEDs and also reduces the aggregation of the final material.[2]

3.2 Chemosensor

As a classic chromophore, pyrene shows interesting fluorescence properties and has been used in chemosensors.[23a,87]Pyrene based AIE/AIEE probe molecules behave as selective and sensitive detectors of metal ions (Cu^{2+}, Fe^{3+} Al^{3+}), picric acid, H^{+} ions etc.[58,66,67,78]

3.3 Organic field-effect transistors (OFET)

The high fluorescence efficiency, electron rich 'macrocyclic' conjugation, and high charge carrier mobility all make pyrene a promising candidate for a variety of organic semiconducting materials.[88] Pyrene-based organic semiconductors have great opportunities in OFETs as charge carrier channel layer materials possessing transport mobility.[8b,87b,89]

3.4 Solid state lasers

Recently, a considerable amount of effort has been devoted to the design of laser materials and devices because of their potential applications.[90] Solid-state laser are comprised of a host and an active ion doped host material. The active ion should have excellent fluorescent, broad absorption bands, high quantum yield etc…, and since pyrene possesses these properties, it is a good candidate for the design and development of new solid-state lasers.

3.5 Biological applications

Pyrene based AIE compounds show good biological activity against both Gram-positive (Rhodococcus rhodochrous and Staphylococcus aureus) and Gram-negative (Escherichia coli and Pseudomonas aeruginosa) bacteria and also fungal species (Candida albicans).[60] Importantly, AIEE probes can sensor M^{3+} ions, and their highly acidic pH sensing ability has been successfully applied in cell imaging and cell viability analysis..[63] The sensitive and selective detection of nucleic acids is important in biological studies, clinical diagnostics, and bio-defence applications and pyrene-based AIEgen have potential in these fields.[91]

3.6 Probing critical micellar concentration (cmc)

The critical micellar concentration (cmc) of both ionic and non-ionic surfactants can conveniently be determined from measurement of the UV absorption of pyrene in surfactant solution. Surfactants can assemble in solution and cmc is an important solution property of surfactants. There are several frequently used methods such as tensiometry, conductometry, fluorimetry and calorimetry, which can be used for its determination.[92] Spectral methods using dyes as probes, and self-absorption of amphiphiles in solution are used for the evaluation of cmc.[93] As fluorescent probes, pyrene molecules has been successfully employed to estimate the polarity level of micelles as well as the cmc of amphiphiles.[94]

4.0 Conclusion

Pyrene is a highly studied fluorophore for a variety of applications. The basis of this review is based on pyrenes ability to emit efficiently in the solid state, and recent reports in the literature revea that is continues to attract the interest of chemists and those involved in materials science and beyond. As a result, much effort has been made to improve the photophysical properties of pyrene. Thus far, the pyrene derivatives that have been reported still present some degree of fluorescence quenching in the solid state. However, scientists are anticipating that more efficient and promising pyrene-based materials with enhanced properties for various uses will be developed through the AIE strategy. By modification at its different site, pyrene could be used in different fields such as an organic light emitting diodes (OLEDs), biosensors, chemosensors, chiral recognition etc as a solid material. This review will be helpful to others and stimulate further investigations into the potential of pyrene-based solid emitters. Such studies will also shed further light on what are the key roles in the AIE or AIEE processes.

Acknowledgements

This work was supported by and the National Natural Science Foundation of China (21602014), and the Youth Fund of Guangdong University of Technology (1108-220413205). M. M. Islam thanks to

This journal is © The Royal Society of Chemistry 20xx

Please do not adjust margins

Please do not adjust margins

MOST, P. R. China for Talented Young Scientist Program (TYSP) Fellowship; CR thanks the EPSRC for an Overseas Travel Grant.

Notes and references

1. (a) S. Tao, Z. Peng, X. Zhang, P. Wang, C. S. Lee and S. T. Lee, *Adv. Funct. Mater*. 2005, **15**, 1716; (b) J. Jayabharathi, P. Jeeva, V. Thanikachalam and S. Panimozhi, *J. Photochem. Photobiol. A Chem.,* 2017, **346**, 296; (c) J. K. Salunke, F. L. Wong, K. Feron, S.Manzhos, M. F. Lo, D. Shinde, A. Patil, C. S. Lee, V. A. L. Roy, P. Sonar and P. P. Wadgaonkar, *J. Mater. Chem. C,* 2016, **4**, 1009; (d) D. Chercka, S.-J. Yoo, M. Baumgarten, J.-J. Kim and K. Müllen, *J. Mater. Chem. C*, 2014, **2**, 9083..
2. M. T. Figueira-Duarte and K. Mullen, *Chem. Rev*. 2011, **111**, 7260.
3. S. Karuppannan andJ. C. Chambron, *Chem Asian J.* 2011, **6**, 964.
4. H. Maeda, T. Maeda, K. Mizuno, K. Fujimoto, H. Shimizu and M. Inouye, *Chem. Eur. J.,* 2006, **12**, 824.
5. Z. Wang, C. Xu, X. Wang, X. Dong, B. Zhao and B. Ji, *Dyes Pigm.,* 2011, **92**, 732.
6. T. Oyamada, H. Uchiuzou, S. Akiyama, Y. Oku, N. Shimoji, K. Matsushige, et al. Lateral organic light-emitting diode with field-effect transistor characteristics. *J. Appl Phys.* **2005**, *98*, 74506.
7. (a) Z. Zhang, B. Xu, J. Su, L. Shen, Y. Xie and H. Tian, *Angew. Chem. Int. Ed.*, 2011, **50***,*11654; (b) Q. Wang, H. Lu, L. Gai, W. Chen, G. Lai andZ. Li, *Dyes. Pigm.,* 2012, **94**, 183; (c) M. Shimizu and T. Hiyama, *Chem Asian J,* 2010, **5**, 1516.
8. (*a*) Z. Li and H. Meng, editors. Boca Raton: CRC Press/Taylor & Francis; 2007; (b) F. Cicoira and C. Santato, *Adv. Funct. Mater.,* 2007, **17**, 3421; (*c*) S. S. Sun, L. R. Dalton, editors. Introduction to organic electronic and optoelectronic materials and devices. Boca Raton: Taylor & Francis; 2008.
9. X. Feng, J.-Y. Hu, C. Redshaw and T. Yamato, *Chem. Eur. J.* 2016, **22**, 11898.
10. (a) J. B. Birks, Photophysics of Aromatic Molecules, Wiley-Interscience, London, 1970; (b) J. R. Lackowicz, Principles of Fluorescence Spectroscopy, Kluwer Academic/Plenum Publishers, New York, 2nd edn, 1999, 595.
11. P. Sonar, M. S. Soh, Y. H. Cheng, J. T. Henssler and A. Sellinger, *Org. Lett.,* 2010, **12**, 3292.
12. (a) M. J. J. Dewar and R. D. Dennington II, *J. Am. Chem. Soc.* 1989, **111**, 3804; (b) H. Cerfontain, K. Laali, H. J. A. Lambrechts, *Recl. Trav. Chim. Pays-Bas* 1983, **102**, 210.
13. (a) X. Luo, J. Li, C. Li, L. Heng, Y. Q. Dong, Z. Liu, Z. Bo and B. Z. Tang, *Adv. Mater.*, 2011, **23**, 3261; (b) H. Tong, Y. Hong, Y. Dong, Y. Ren, M. Haussler, J. W. Y. Lam, K. S. Wong and B. Z. Tang, *J. Phys. Chem. B*, 2007, **111**, 2000.
14. G. Venkataramana andS. Sankararaman, *Eur. J. Org. Chem.,* 2005,**19**, 4162.
15. (a) C. Lambert, J. Ehbets, D. Rausch and M. Steeger, *J. Org. Chem.,* 2012, **77**, 6147; (b) L. Ji, R. M. Edkins, A. Lorbach, I. Krummenacher, C. Brückner, A. Eichhorn, H. Braunschweig, B. Engels, P. J. Low and T. B. Marder, *J. Am. Chem. Soc.*, 2015, **137**, 6750; (c) A. G. Crawford, A. D. Dwyer, Z. Liu, A. Steffen, A. Beeby, L.-O. Pålsson, D. J. Tozer and T. B. Marder, *J. Am. Chem. Soc.,* 2011, **133**, 13349.
16. Wanninger-Weiß and H.-A. Wagenknecht, *Eur. J. Org. Chem.*, 2008, 64.
17. (a) J. Wang, Y. Zhao, C. Dou, H. Sun, P. Xu, K. Ye, J. Zhang, S. Jiang, F. Li, Y. Wang, *J Phys. Chem. B,* 2007, **111**, 5082; (b) S. Hecht and J. M. J. Fr_echet, *Angew. Chem. Int. Ed.* 2001, **40**, 74; (c) B. T. Nguyen, J. E. Gautrot, C. Y. Ji, P. L. Brunner, M. T. Nguyen and X. X. Zhu, *Langmuir*, 2006, **22**, 4799.
18. (a) D. Y. Kim, H. N. Cho and C. Y. Kim, *Prog. Polym. Sci.,* 2000, **25**, 1089; (b) C. T. Chen, *Chem. Mater.,* 2004, **16**, 4389.
19. (a) K. A. Zachariasse, *Trends Photochem. Photobiol*., 1994, **3**, 211; (b) J. B. Birks, D. J. Dyson and I. H. Munro, *Proc. R. Soc. London, Ser. A,*1963, **275**, 575.
20. (a) J. A. Mikroyannidis, L. Fenenko and C. Adachi, *J. Phys. Chem. B*, 2006, **110**, 20317; (b) Z.-Q. Liang, Y.-X. Li, J.-X. Yang, Y. Ren, X.-T. Tao, *Tetrahedron Lett.*, 2011, **52**, 1329; (d) C. Tang, F. Liu, Y.-J. Xia, L.-H. Xie, A. Wei, S.-B. Li, Q.-L. Fan and W. Huang, *J. Mater. Chem.,* 2006, **16**, 4074.
21. W. Z. Yuan, P. Lu, S. M. Chen, J. W. Y. Lam, Z. M. Wang, Y. Liu, H. S. Kwok, Y. G. Ma and B. Z. Tang, *Adv. Mater.,* 2010, **22**, 2159.
22. (a) Wu, K. C.; Ku, P. J.; Lin, C. S.; Shih, H. T.; Wu, F. I.; Huang, M. J.; Lin, J. J.; Chen, I.-C.; Cheng, C. H. *Adv. Funct. Mater.,* 2008, **18**, 67; (b) T. M. Figueira-Duarte, P. G. Del Rosso, R. Trattnig, S. Sax, E. J. W. List and K. Müllen, *Adv. Mater.* 2009, **21**, 1.
23. (a) F. M. Winnik, *Chem. Rev.,* 1993, **93**, 587; (b) G. Venkataramana and S. Sankararaman, *Org. Lett.,* 2006, **8**, 2739; (c) V. de Halleux, J.-P.Calbert, P. Brocorens, J. Cornil, J.-P.Declercq, J. L.Bredas and Y. Geerts, *Adv. Funct. Mater*. 2004, **14**, 649; (d) D. Rausch and C. Lambert, *Org. Lett.*, 2006, **8**, 5037. (e) J.-Y. Hu, X. Feng, A. Paudel, H. Tomiyasu, U. Rayhan, P. Thuery, M. R. J. Elsegood, C. Redshaw, T. Yamato, *Eur. J. Org. Chem.* 2013, 5829. (f) X. Feng, J.-Y. Hu, L. Yi, N. Seto, Z. Tao, C. Redshaw, M. R. J. Elsegood, T. Yamato, *Chem. Asian J.* 2012, **7**, 2854. (g) X. Feng, J.-Y. Hu, F. Iwanaga, N. Seto, C. Redshaw, M. R. J. Elsegood, *Org. Lett.* 2013, **15**, 1318. (h) Y. Qiao, J. Zhang, W. Xua, D. Zhu, *Tetrahedron* 2011, **67**, 3395.
24. I. B. Berlman, *J. Phys. Chem.* 1970, **74**, 3085.
25. (a) J. Luo, Z. Xie, J.W. Y. Lam, L. Cheng, H. Chen, C. Qiu, H. S. Kwok, X. Zhan, Y. Liu, D. Zhu and B. Z. Tang, *Chem. Commun.* **2001**, 1740; (b) Y. Hong, J. W. Y. Lam and B. Z. Tang, *Chem. Commun.*, 2009, 4332; (c) Y. Hong, J. W. Y. Lam and B. Z. Tang*, Chem. Soc. Rev.*, 2011, **40**, 5361; (d) J. Mei, Y. Hong, J. W. Y. Lam, A. Qin, Y. Tang and B. Z. Tang, *Adv. Mater.*, 2014, **26**, 5429; (e) R. Hu, N. L. C. Leung and B. Z. Tang, *Chem. Soc. Rev*., 2014, **43**, 4494.
26. (a) J. Chen, C. C. W. Law, J. W. Y. Lam, Y. Dong, S. M. F. Lo, I. D. Williams, D. Zhu, B. Z. Tang, *Chem. Mater.,* 2003, **15**, 1535; (b) J. Mei, N. L. C. Leung, R. T. K. Kwok, . W. Y. Lam and Ben Z. Tang, *Chem. Rev.,* 2015, **115**, 11718.

Please do not adjust margins

Please do not adjust margins

27. H. Shi, R. T. K. Kwok, J. Liu, B. Xing, B. Z. Tang and B. Liu, *J. Am. Chem. Soc.,* 2012, **134**, 17972.
28. Y. Wang, T. Liu, L. Bu, J. Li, C. Yang, X. Li, Y. Tao and W. Yang, *J. Phys. Chem. C,* 2012, **116**, 15576.
29. B. K. An, S. K. Kwon, S. D. Jung and S. Y. Park, *J. Am. Chem. Soc.,*2002, **124**, 14410.
30. Y. Li, F. Li, H. Zhang, Z. Xie, W. Xie, H. Xu, B. Li, F. Shen, L. Ye, M. Hanif, D. Ma and Y. Ma, *Chem. Commun.* 2007, 231.
31. Y. Dong, J. W. Y. Lam, A. Qin, Z. Li, J. Sun, H. H. Y. Sung, I. D. Williams and B. Z. Tang, *Chem. Commun.,* 2007, 40.
32. R. Deans, J. Kim, M. R. Machacek and T. M. Swager, *J.Am. Chem. Soc.,* 2000, **122**, 8565.
33. K. Perumal, J. A. Garg, O. Blacque, R. Saiganesh, S. Kabilan, K. K. Balasubramanian and K. Venkatesan, *Chem.–Asian J.,* 2012,**7**, 2670.
34. J. Wang, J. Mei, R. Hu, J. Z. Sun, A. Qin and B. Z. Tang, *J. Am. Chem. Soc.,* 2012, **134**,9956.
35. N. B. Shustova, B. D. McCarthy and M. Dinca, *J. Am. Chem. Soc.* 2011, **133**, 20126.
36. B. Manimaran, P. Thanasekaran, T. Rajendran, R. J. Lin, I. J. Chang, G. H. Lee, S. M. Peng, S. Rajagopal and K. L. Lu, *Inorg. Chem*., 2002, **41**, 5323.
37. B. Pramanik and D. Das, J. *Phys. Chem. C,* 2018, **122**, 3655.
38. (a) R. J. Argauer, White CE, Fluorescent compounds for calibration of excitation and emission units of spectrofluorometer, *Anal Chem*, 1964; (b) C. A. Royer, *Biophys. J.,* 1995, 1191 (c) M. R. Eftink, *Biophys. J.*, 1994, **66**, 482; (d) S.-J. Kim, F. N. Chowdhury, W. Stryjewski, E. S. Younathan, P. S. Russo and M. D. Barkley, *Biophys. J.,* 1993, **65**, 215-226.
39. Q. Wang, H. Liu, H. Lu, Z. Xu, G. Lai, Z. Li, J. Mack and Z. Shen, *Dyes. Pigm.,*2013, **99**, 771.
40. Z. J. Zhao, S. M. Chen, J. W. Y. Lam, P. Lu, Y. C. Zhong, K. S. Wong, H. S. Kwok and B. Z. Tang, *Chem. Commun.*, 2010, **46**, 2221.
41. (a) J. Yang, J. Huang, N. Sun, Q. Peng, Q. Li, D. Ma and Z. Li, *Chem. Eur. J.,* 2015, **21**, 6862; (b) J. Yang, L. Li, Y. Yu, Z. Ren, Q. Peng, S. Ye, Q. Li and Z. Li, *Mater. Chem. Front.,* 2017, **1**, 91.
42. X. Feng, C. Qi, H.-T. Feng, Z. Zhao, H. H. Y. Sung, I. D. Williams, R.T. K. Kwok, J. W. Y. Lam, A. Qin and B. Z. Tang, *Chem. Sci.*, 2018, **9**, 5679.
43. (a) C. Y. K. Chan, J. W. Y. Lam, J. Zhao, S. M. Chen, P. Lu, H. H. Y. Sung, H. S. Kwok, Y. Ma, I. D. Williams and B. Z. Tang, *J Mater Chem C*, 2014, **2**, 4320; (b) T. Jadhav, J. M. Choi, J. Y. Lee, B. Dhokale, R. Misra, *Org Electron* 2016, **37**, 448; (c) T. Jadhav, B. Dhokale, Y. Patil, S. M. Mobin, R. Misra, *J. Phys. Chem. C,* 2016, **120**, 24030.
44. (a) Y. Liu, Y. Tang, N. N. Barashkov, I. S. Irgibaeva, J. W. Y. Lam, R. Hu, D. Birimzhanova, Y. Yu and B. Z. Tang, *J. Am. Chem. Soc.,* 2010, **132**,13951; (b) L. Chen, Y. Jiang, H. Nie, R. Hu, H. S. Kwok, F. Huang, A. Qin, Z. Zhao and B. Z. Tang, *ACS Appl. Mater. Interfaces* 2014, **6**, 17215.
45. (a) Y. Liu, S. Chen, J. W. Y. Lam, P. Lu, T. K. Kwok, F. Mahtab, H. S. Kwok and B. Z. Tang, *Chem Mater.,* 2011, **23**, 2536; (b) Z. Zhao, P. Lu, J. W. Y. Lam, Z. Wang, C. Y. K. Chan, H. H. Y. Sung, I. D. Williams, Y. Ma and B. Z. Tang, *Chem. Sci.*, 2011,**2**, 672.
46. (a) Z. Zhao, S. Chen, J. W. Y. Lam, Z. Wang, P. Lu, F. Mahtab, H. H. Y. Sung, I. D. Williams, Y. Ma, H. S. Kwok and B. Z. Tang, *J. Mater. Chem.,* 2011, **21**, 7210;(b) W. Wang, T. Lin, M. Wang, T.-X. Liu, L. Ren, D. Chen and S. Huang,*J. Phys. Chem. B,* 2010, **114**, 5983; (c) D. Jana, S. Boxi and B. K. Ghorai, *Dyes Pigm.,* 2013, **99**, 740.
47. Z. Zhang, Y. Zhao, R. Zhang, L. Zhang, W. Cheng and Z. H. Ni*, Dyes Pigm.,* 2015, **118**, 95.
48. J. Yang, Q. Guo, X. Wen, X. Gao, Q. Peng, Q. Li, D. Ma andZ. Li, *J. Mater. Chem. C,* 2016, **4**,8506.
49. J. Yang, J. Qin, Z. Ren, Q. Peng, G. Xie and Z.Li, *Molecules,* 2017, **22**, 2144.
50. S. Son, A. Dodabalapur, A. J. Lovinger and M. E. Galvin, *Science*, 1995, **269**, 376.
51. (a) B. Wang, Y. Wang, J. Hua, Y. Jiang, J. Huang, S. Qian andH. Tian, H. *Chem. Eur. J.,* 2011, **17**, 2647; (b) B. Gao, H. Wang, Y. Hao, L. Fu, H. Fang, Y. Jiang, L. Wang, Q. Chen, H. Xia, L. Pan, Y. Ma and H. Sun, *J. Phys. Chem. B,* 2010, **114**, 128; (c) Z. Wang, H. Shao, J. Ye, L. Tang and P. Lu, *J. Phys. Chem. B*, 2005, **109**, 19627; (d) J. N. Wilson, M. D. Smith, V. Enkelmann and U. H. F. Bunz, *Chem. Commun.*, 2004, 1700; (e) C. J. Bhongale, C.-S. Chang, C.-S. Lee, E. W.-G. Diau and C.-S. Hsu, *J. Phys. Chem. B*, 2005, **109**, 13472; (f) H. Tong, Y. Dong, M. Häußler, Y. Hong, J. W. Y. Lam, H. H.-Y.Sung, I. D.Williams, H. S. Kwok and B. Z. Tang, *Chem. Phys. Lett.,* 2006, **428**, 326; (g) P. An, Z. Shi, W. Dou, X. Cao and H. Zhang, *Org. Lett*., 2010, **12**, 4364.
52. Y.-X. Li, G.-X. Sun, J.-L. Miao, Y. Nie, Z.-W. Zhang and X.- T. Tao, *Tetrahedron Lett*., 2013, **54**, 3263.
53. Y.-X. Li, X.-F. Yang, J.-L. Miao and G.-X. Sun, *J. Phys. Chem. C,* 2016, **120**, 21722.
54. J. Katla, H. R. Bhat, P. C. Jha, P. S. Ghalsasi and S. Kanvah, *ChemistrySelect*, 2017, **2**, 1902.
55. A. D. Aleo, A. Karapetyan, V. Heresanu, M. Giorgi and F. Fages, *Tetrahedron,*2015, **71**, 2255.
56. A. Karuppusamy, T. Vandana and P. Kannan, *J. Photochem. Photobiol. A Chem.,* 2017, **345**, 11.
57. (a) D. A. Pearce, N. Jotterand, I. S. Carrico and B. Imperiali, *J. Am. Chem. Soc.,* 2001, **123**, 5160; (b) M. Mameli, M. C. Aragoni, M. Arca, C. Caltagirone, F. Demartin, G. Farruggia, G. D. Filippo, F. A. Devillanova, A. Garau, F. Isaia, V. Lippolis, S. Murgia, L. Prodi, A. Pintus and N. Zaccheroni, *Chem.–Eur. J.,* 2010, **16**, 919; (c) Y. Bao, B. Liu, H. Wang, F. Du and R. Bai, *Anal. Methods.,* 2011, **3**, 1274; (d) Y. Bao, B. Liu, F. Du, J. Tian, H. Wang and R. Bai, *J. Mater. Chem.,* 2012, **22**, 5291.
58. M. Shellaiah, Y.-H. Wu, A. Singh, M. V. R. Raju and H.-C. Lin, *J. Mater. Chem. A*, 2013, **1**, 1310.
59. (a) D. T. McQuade, A. E. Pullen and T. M. Swager, *Chem. Rev.,* 2000, **100**, 2537; (b) G. Aragay, J. Pons and A. Merkoci, *Chem. Rev.,* 2011, **111**, 3433.
60. A. Kathiravan, K. Sundaravel, M. Jaccob, G. Dhinagaran, A. Rameshkumar, D. A. Ananth and T. Sivasudha, *J. Phys. Chem.B,* 2014, **118**, 13573.

 This journal is © The Royal Society of Chemistry 20xx

Please do not adjust margins

Please do not adjust margins

61. Y. Li, W. Huang, J. Yong, S. Huang, Y. Li, Y. Liu and D. Wu, *New J. Chem.,* 2018, **42**, 12644.
62. Q. Chai, J. Wei, B. Bai, H. Wang and M. Li, *Dyes Pigm.,* 2018, **152**, 93.
63. M. Shellaiah, T. Simon, V. Srinivasadesikan, C.-M. Lin, K. W. Sun, F.-H. Ko, M.-C. Lin and H.-C. Lin, *J. Mater. Chem. C,* 2016, **4**, 2056.
64. J. E. Kwon and S. Y. Park. *Adv. Mater.,* 2011, **23**, 3615.
65. S. Samanta, U. Manna and G.l Das, *New J. Chem.***,** 2017, **41**, 1064.
66. M. Shyamal,P. Mazumdar,S. Maity,G. P. Sahoo,G. Salgado-Morán and A. Misra, *J. Phys. Chem. A,* 2016, **120**, 210.
67. M. Shyamal, S. Maity, P. Mazumdar, G. P. Sahoo, R. Maity and A. Misra, *J. Photochem. Photobiol. A Chem.,* 2017, **342**, 1.
68. T. Jadhav, B. Dhokale, S. M. Mobin and R. Misra, *J. Mater. Chem. C,* 2015, **3**, 9981.
69. Y. Liu, T. Shan, L. Yao, Q. Bai, Y. Guo, J. Li, X. Han, W. Li, Z. Wang, B. Yang, P. Lu and Y. Ma, *Org. Lett.* 2015, **17**, 6138.
70. Y. Sagara, T. Mutai, I. Yoshikawa and K. Araki, *J. Am. Chem. Soc.,* 2007, **129**, 1520.
71. b) Y. Sagara, T. Kato, *Angew. Chem. Int. Ed.,* **2008**, *47*, 5175; c) M. J. Teng, X. R. Jia, S. Yang, X. F. Chen, Y. Wei, *Adv. Mater.* **2012**, *24*, 1255; d) M. J. Teng, X. R. Jia, X. F. Chen, Y. Wei, *Angew. Chem. Int. Ed.* **2012**, *51*, 6398; e) T. S. Wang, N. Zhang, K. Zhang, J. W. Dai, W. Bai, R. K. Bai, *Chem. Commun.,* 2016, **52**, 9679.
72. L. Ji, A. Lorbach, R. M. Edkins and T. B. Marder, *J. Org. Chem.,* 2015, **80**, 5658.
73. (a) L. Zöphel, D. Beckmann, V. Enkelmann, D. Chercka, R. Rieger and K. Müllen, *Chem. Commun*., 2011, **47**, 6960; (b) T. Yamato, M. Fuimoto, A. Miyazawa and K. Matsuo, *J. Chem. Soc., Perkin Trans. 1,* 1997, 1201; (c) B. Kohl, F. Rominger and M. Mastalerz, *Angew. Chem., Int. Ed.,* 2015, **54**, 6051; (d) H. M. Duong, M. Bendikov, D. Steiger, Q. Zhang, G. Sonmez, J. Yamada and F. Wudl, *Org. Lett.*, 2003, **5**, 4433; (e) K. Baumgärtner, K. A. L. M. Chincha, A. Dreuw, F. Rominger and M. Mastalerz, *Angew. Chem., Int. Ed.*, 2016, **55**, 1.
74. (a) L. Zöphel, V. Enkelmann and K. Müllen, *Org. Lett.,* 2013, **15**, 804; (b) S. N. Keller, N. L. Veltri and T. C. Sutherland, *Org. Lett.*, 2013, **15**, 4798;. (b) M. Piotrowicz, J. Zakrzewski, R. Métivier, A. Brosseau, A. Makal and K. Woźniak, *J. Org. Chem.*, 2015, **80**, 2573.
75. S. Sasaki, S. Suzuki, K. Igawa, K. Morokuma and G.-I Konishi, , *J. Org. Chem.,* 2017, **82**, 6865.
76. V. Kachwal, P. Alam, H. R. Yadav, S. S. Pasha, A. R. Choudhury and I. R. Laskar, *New J. Chem.*, 2018,**42**, 1133.
77. U. K.Das and P. Dastidar, *J. Chem. Sci.,* 2014, **126**, 1357.
78. K. Nishino, H. Yamamoto, K. Tanaka and Y. Chujo, *Org. Lett*., 2016, **18**, 4064.
79. V. Vij, V. Bhalla and M. Kumar, *Chem. Rev.* 2016, **116**, 9565.
80. C.-Z. Wang, Y. Noda, C. Wu, X. Feng, P. Venkatesan, H. Cong, M. R. J. Elsegood, T. G. Warwick, S. J. Teat, C. Redshaw, T. Yamato, *Asian J. Org. Chem.* 2018,**7**, 444.
81. (a) Y. Niko, S. Kawauchi, S. Otsu, K. Tokumaru and G.-I. Konishi, *J. Org. Chem.,* 2013, **78**, 3196; (b) Y. Niko, Y. Cho, S. Kawauchi and G.-I. Konishi, *RSC Adv.,* 2014, **4**, 36480.
82. (a) A. Matsumoto, M. Suzuki, D. Kuzuhara, J. Yuasa, T. Kawai, N. Aratani and H. Yamada, *Chem. Commun.,* 2014, **50**, 10956; (b) H. Lee, B. Kim, S. Kim, J. Kim, J. Lee, H. Shin, J. Lee and J. Park, *J. Mater. Chem. C*, 2014, **2**, 4737.
83. (a) J. N. Moorthy, P. Natarajin, P. Venkatakrishnan, D. F. Huang and T. J. Chow, *Org. Lett.*, 2007, **9**, 5215; (b) M. Y. Lo, C. G. Zhen, M. Lauters, G. E. Jabbour and A. Sellinger, *J. Am. Chem. Soc.,* 2007, **129**, 5808; (C) R. D. Xia, W. Y. Lai, P. A Levermore, W. Huang and D. D. C. Bradley, *Adv. Funct. Mater.,* 2009, **19**, 2844; (d) Z. J. Zhao, J. H. Li, X. P. Chen, X. M. Wang, P. Lu and Y. Yang, *J. Org. Chem.,* 2009, **74**, 383.
84. (a) H. J. Zhang, Y. Wang, K. Z. Shao, Y. Q. Liu, S. Y. Chen, W. F. Qiu, X. B. Sun, T. Qi, Y. Q. Ma, G. Yu, Z. M. Su and D. B. Zhu, *Chem. Commun.,* 2006, 755; (b) M. J. Sienkowska, J. M. Farrar, F. Zhang, S. Kusuma, P. A. Heiney and P. Kaszynski, *J. Mater. Chem*., 2007, **17**, 1399; (c) F. Liu, W. Y. Lai, C. Tang, H. B. Wu, Q. Q. Chen, B. Peng, W. Wei, W. Huang and Y. Cao, *Macromol. Rapid Commun.,* 2008, **29**, 659.
85. X. Feng,Z. Xu,Z. Hu, C. Qi, D. Luo, X. Zhao, Z. Mu,C. Redshaw, J. W. Y. Lam, D. Ma and B. Z. Tang, *J. Mater. Chem. C*, 2019, DOI: 10.1039/C8TC05547E.
86. N. J. Jeon, J. Lee, J. H. Noh, M. K. Nazeeruddin, M. Grätzel and S. Seok, *J. Am. Chem. Soc*., 2013, **135**, 19087.
87. (a) J. R. Lakowicz, Principles of Fluorescence Spectroscopy; Springer: New York, 2006; (b) W. Z. Yuan, S. Chen, J.W. Y. Lam, C. Deng, P. Lu, H. H. Y. Sung, I. D. Williams, H. S. Kwok, Y. Zhang and B. Z. Tang, *Chem. Commun*., 2011, 11216;; (c) C. Shi, Z. Guo, Y. Yan, S. Zhu, Y. Xie, Y. S. Zhao, W. Zhu and H. Tian, H. *ACS Appl. Mater. Interfaces,* 2013, **5**, 192.
88. (a) X. Gao and Z. Zhao, *Sci China Chem*, 2015, **58**, 947; (b) K. Oniwa, H. Kikuchi, H. Shimotani, S. Ikeda, N. Asao, Y. Yamamoto, K. Tanigaki and T. Jin, *Chem Commun*, 2016, **52**, 4800; (c) F. Moggia, C. Videlot-Ackermann. J. Ackermann, P. Raynal, H. Brisset and F. Fages, *J Mater Chem.*, 2006, **16**, 2380; (d) J. E. Anthony, *Angew Chem Int Ed*, 2008, **47**, 452.
89. J. Zaumseil and H. Sirringhaus, *Chem. Rev.,* 2007, **107**, 1296.
90. (a) X. J. Tang, L. Z. Wu, L. P. Zhang and C. H. Tung, *Chem. Phys. Lett.* 2002, **356**, 573; (b) G. S. He, T. C. Lin, V. K. S. Hsiao, A. N. Cartwright, P. N. Prasad, L. V. Natarajan, V. P. Tondiglia, R. Jakubiak, R. A. Vaia and T. J. Bunning, *Appl. Phys. Lett*., 2003, **83**, 2733.
91. J. Huang, Y. Wu, Y. Chen, Z. Zhu, X. Yang, C. J. Yang, K. Wang and W. Tan, *Angew. Chem. Int. Ed.* 2011, **50**, 401.
92. J.H. Clint, Surfactant Aggregation: Blacki, Chapman and Hall, New York, 1991.
93. (a) S. K. Hait, P. R. Majhi, A. Blume and S. P. Moulik, *J. Phys. Chem. B,* 2003, **107**, 3650; (b) M. Prasad, A. MacDonald, R. Palepu, S. P. Moulik and J. Surf. *Sci. Technol.,* 2003,**19**, 125.

Please do not adjust margins

Please do not adjust margins

94. (a) G. B. Ray, I. Chakraborty and S. P. Moulik, *J. Colloid Interface Sci.,* 2006, **294**, 248; (b) K. Kalyansundaran and J. K. Thomas, *J. Am. Chem. Soc.,* 1977, **99**, 2039; (c) J. Aguiar, P. Carpana, J. A. Molina-Boliver and C. C. Ruiz, *J. Colloid Interface Sci.,* 2003, **258**, 116.

 This journal is © The Royal Society of Chemistry 20xx

Please do not adjust margins